Am J Physiol Heart Circ Physiol 302: H51–H68, 2012.
First published October 7, 2011; doi:10.1152/ajpheart.00358.2011.

Wall structures of myocardial precapillary arterioles and postcapillary venules reexamined and reconstructed in vitro for studies on barrier functions

Stephan Nees,[1]* Gerd Juchem,[2]* Nicola Eberhorn,[1] Martin Thallmair,[1] Stefan Förch,[1] Maria Knott,[1] Anton Senftl,[1] Theodor Fischlein,[4] Bruno Reichart,[2] and Dominik R. Weiss[3]

Departments of [1]Physiology and [2]Cardiac Surgery, University of Munich, Munich; [3]Department of Transfusion Medicine and Hemostaseology, University of Erlangen-Nuremberg, Erlangen; and [4]Department of Cardiac Surgery, Hospital Nuremberg South, Nuremberg, Germany

Submitted 11 April 2011; accepted in final form 3 October 2011

Nees S, Juchem G, Eberhorn N, Thallmair M, Förch S, Knott M, Senftl A, Fischlein T, Reichart B, Weiss DR. Wall structures of myocardial precapillary arterioles and postcapillary venules reexamined and reconstructed in vitro for studies on barrier functions. *Am J Physiol Heart Circ Physiol* 302: H51–H68, 2012. First published October 7, 2011; doi:10.1152/ajpheart.00358.2011.—The barrier functions of myocardial precapillary arteriolar and postcapillary venular walls (PCA or PCV, respectively) are of considerable scientific and clinical interest (regulation of blood flow and recruitment of immune defense). Using enzyme histochemistry combined with confocal microscopy, we reexamined the cell architecture of human PCA and PVC and reconstructed appropriate in vitro models for studies of their barrier functions. Contrary to current opinion, the PCA endothelial tube is encompassed not by smooth muscle cells but rather by a concentric layer of pericytes cocooned in a thick, microparticle-containing extracellular matrix (ECM) that contributes substantially to the tightness of the arteriolar wall. This core tube extends upstream into the larger arterioles, there additionally enwrapped by smooth muscle. PCV consist of an inner layer of large, contractile endothelial cells encompassed by a fragile, wide-meshed pericyte network with a weakly developed ECM. Pure pericyte and endothelial cell preparations were isolated from PCA and PCV and grown in sandwich cultures. These in vitro models of the PCA and PCV walls exhibited typical histological and functional features. In both plasma-like (PLM) and serum-containing (SCM) media, the PCA model (including ECM) maintained its low hydraulic conductivity (L_P = 3.24 ± 0.52·10^{-8}cm·s^{-1}·cmH$_2$O^{-1}) and a high selectivity index for transmural passage of albumin (SI_{Alb} = 0.95 ± 0.02). In contrast, L_P and SI_{Alb} in the PCV model (almost no ECM) were 2.55 ± 0.32·10^{-7}cm·s^{-1}·cmH$_2$O^{-1} and 0.88 ± 0.03, respectively, in PLM, and 1.39 ± 0.10·10^{-6}cm·s^{-1}·cmH$_2$O^{-1} and 0.49 ± 0.04 in SCM. With the use of these models, systematic, detailed studies on the regulation of microvascular barrier properties now appear to be feasible.

pericytes; coronary system; tissue factor; endothelial cells; inflammation

THE EXTENSIVE HISTOLOGICAL literature presents an apparently clear picture with respect to the structure of myocardial arterioles: while those with a diameter >20 μm (muscular arterioles) consist of an inner tube of continuous endothelium surrounded by two or more concentric layers of smooth muscle cells (SMC), the far more frequent precapillary arterioles (endarterioles) have only one layer of SMC encompassing the endothelial core tube (28, 64).

Given not only the large numbers, but also their outstanding sensitivity to numerous vasoactive hormones and neurotransmitters and their far greater surface area in contact with the blood and interstitial fluid, the precapillary arterioles represent especially prominent controlling elements in the regulation of myocardial blood flow (21, 24, 29). In this context, endothelially mediated mechanisms (60) play a key functional role, although the fundamental details of these mechanisms are still incompletely understood. It has long been known, for instance, that a variety of vasoactive substances, all very hydrophilic (e.g., acetylcholine), act as vasodilators when present intraluminally but as vasoconstrictors when in direct contact with the SMC. This seemingly paradoxical effect finally led to the discovery of endothelium-derived relaxing factor (EDRF), a soluble autacoid of initially unknown structure (16, 47). Clearly, if luminally present hydrophilic vasodilators cannot mediate their vasodilatory effect on the SMC by themselves, their access to these cells must be prevented by a dense, probably partly hydrophobic tissue barrier, while access of EDRF must be allowed. Although EDRF was subsequently identified as the small lipophilic and therefore extremely rapidly diffusible gas molecule nitric oxide (6), the properties of the intramural diffusion barrier remained undefined. In any event, from the extensively studied structure of the complex blood-brain barrier, it is clear that the endothelial tissue layer alone is not an effective structural barrier to the diffusion of small hydrophilic substances from the blood into the interstitium, even when the respective continuous endothelium is characterized by well-organized and numerous tight junctions like the endothelium of the brain in all the microvascular provinces of this complex organ (9).

The capillaries aborizing from the endarterioles merge with the venous capillaries and the latter form the tributaries of the myocardial postcapillary venules. The continuum of this enormously extended postcapillary venular system (22, 33, 35, 44, 75) in muscular tissue has a surface area in contact with the blood that is at least as large as that of the arterial capillary networks. In a 250-g human heart, for instance, the total capillary surface area is ~13 m^2 (recalculated from Ref. 4). While the arteriolar capillary limb subserves the exchange of low-molecular-weight solutes and gases between the intravascular and interstitial spaces, the endothelial exchange area of the postcapillary venular system is generally designed for the rapid recruitment of the large protein molecules and cellular components of the immune system from the blood into inflamed areas (1, 25). Indeed, postcapillary venules have a particularly responsive endothelium [postcapillary venular endothelium (PVE)] that, shortly after contact with inflammatory

* S. Nees and G. Juchem contributed equally to this work.

Address for reprint requests and other correspondence: S. Nees, Dept. of Physiology, Univ. of Munich (LMU), Schillerstr. 44, 80336 Munich, Germany (e-mail: stephan.nees@lrz.uni-muenchen.de or: stephan@snees.de).

mediators, alters its typical morphology (68) characteristically, finally closely resembling the "high venular endothelium" in the lymph nodes (58). In parallel, the intercellular junctions of the activated PVE, already relatively loose compared with those of the arterioles (12), open widely under the influence of certain inflammatory mediators. Given a thin venular basement membrane (72), and that the subendothelial pericytes, particularly numerous in the venules (69), form only a widely meshed net, even high-molecular-weight plasma proteins can be flushed into the interstitium, resulting in inflammatory edema (25) and often also interstitial fibrin clots. The activated PVE, moreover, expresses a multitude of adhesion molecules (42, 51, 55) to which blood leukocytes adhere and initiate their diapedesis.

Although detailed investigation of precapillary arteriolar and postcapillary venular barrier functions is clearly of considerable basic and clinical interest, their direct investigation is restricted in intact heart tissue due to the severely limited experimental access. On the other hand, the substantial advances in the investigation of the blood-brain barrier (5, 45) show that considerable progress in the elucidation of vascular barrier functions can be achieved using appropriate in vitro models constructed by cultivating defined wall tissues of specific microvascular segments in "sandwich style" (50, 76).

We therefore developed new methods for the selective isolation of bulk amounts of human myocardial precapillary arterioles and postcapillary venules, reinvestigated their cell architecture, and developed suitable in vitro models for the quantitative investigation of the barrier functions of the respective microvascular walls. Contrary to current opinion, the endothelial tube of the most important resistance vessels of the heart, the precapillary arterioles, is encompassed not by SMC but rather by a concentric layer of pericytes cocooned in thick, microparticle-containing extracellular matrix (ECM). The latter contributes substantially to the tightness of the precapillary arteriolar vessel wall. In fact, initial in vitro studies showed that the precapillary arteriolar wall model is characterized by a remarkably low hydraulic conductivity (L_P) and high albumin transport selectivity regardless of the incubation conditions chosen. The venular model, in contrast, increased its L_P rapidly and lowered its albumin transport selectivity substantially on exposure to inflammatory mediators, which are naturally always present in serum-containing media.

MATERIALS AND METHODS

Materials

Polymorphoprep was obtained from Axis-Shield (Oslo, Norway); Biseko, a commercially available plasma derivative free of isoagglutinines and coagulation factors was from Biotest AG (Dreieich, Germany); Transwell polyethyleneterephthalat culture devices with a surface area of 4.5 cm^2, a pore size of 0.4 μm, and a pore density of $10^8/cm^2$ were from Corning (Corning, NY); Percoll was from GE Healthcare Europe (Freiburg, Germany); DMEM, FCS, streptomycin, penicillin, balanced salt solution (BSS), PBS, trypsin/EDTA, and human endothelial serum-free media (SFM) basal growth medium were from Invitrogen (Karlsruhe, Germany); secondary antibodies (highly cross-adsorbed, if available) conjugated with Alexa Fluor 488 or 546, and DiI-acLDL were from Molecular Probes (Eugene, OR); endothelial cell growth medium (ECGM) was from Promocell (Heidelberg, Germany); collagenase B and dispase II were purchased from Roche Diagnostics (Mannheim, Germany); antibodies against β-receptor for platelet-derived growth-factor, NG2, and VE-cadherin were from Santa Cruz (Heidelberg, Germany); anti-human CD 31 [platelet endothelial cell adhesion molecule (PECAM), mouse monoclonal] was obtained from Serotec (Oxford, UK); Ficoll 70, gly-Pro-4-methoxy-β-naphthylamide, Fast blue B, naphthol-AS-MX-phosphate dinatrium salt, Fast Blue BB ½ $ZnCl_2$, Fast Red TR, endothelial-SFM basal growth medium, highly purified BSA, anti-α-smooth muscle actin (murine monoclonal IgG, clone 1A4), and anti-von Willebrand factor antigen (rabbit polyclonal) were purchased from Sigma (St. Louis, MO); anti-human tissue factor (TF; polyclonal rabbit) was from American Diagnostica (Stamford, CT); and nylon membrane filters (90-mm diam., 20-μm pore size) were obtained from Sterlitech (Kent, WA).

Solutions

All weight percentages refer to wt/vol. Solutions were as follows: 1% BSA in PBS (PBS-A); BSS (in mM): 140 NaCl, 5.4 KCl, 1.0 NaH_2PO_4, and 0.8 $MgSO_4$; Ca^{2+}-free Ringer solution (in mM): 127 NaCl, 4.6 KCl, 1.1 $MgSO_4$, 1.2 KH_2PO_4, 25 $NaHCO_3$, 7.6 glucose, 2 pyruvate, 10 creatine, 20 taurine, 5 ribose, 2 aspartic acid, 2 glutamic acid, 1 arginine, and 0.5 uric acid, equilibrated with 95% CO_2-5% O_2; and protease solution: 0.09% collagenase B, 0.012% dispase II (Roche), and 0.2% highly purified BSA. These proteins were dissolved in Ringer solution and subsequently sterilized by filtration through a sterile filter (pore size of 0.22 μm); mixed culture medium: mixture of equal volumes of DMEM and ECGM, adjusted to 6% (vol/vol) FCS and supplemented with 200 U/ml penicillin and 0.2 mg/ml streptomycin; human endothelial culture medium: human endothelial SFM basal growth medium supplemented with 10% FCS (vol/vol), 200 U/ml penicillin, 0.2 mg/ml streptomycin, 1 μg/ml fibronectin, 10 ng/ml EGF, and 20 ng/ml FGF; filtration medium: 7 vol serum-free ECGM mixed with 3 vol Biseko. Before use, the latter was dialyzed extensively against freshly prepared human citrate plasma supplemented with 10.000 U/ml penicillin and 10 μg/ml streptomycin. Finally, the dialysate was adjusted to a concentration of free calcium ions of 4 mM, centrifuged for 1 h at 15.000 *g*, and filtered freshly before use (pore size 0.22 μm).

Methods

Human cell and tissue preparations. All experiments with human cells and tissues were performed after obtaining the written informed consent of the patients and approval of the ethics committee of the Ludwig-Maximilians-University (LMU) of Munich according to the principles expressed in the Declaration of Helsinki.

Histological techniques. FIXATION. Collected vascular segments obtained after filtration of proteolytically dispersed ventricular tissue were spread on the bottom of Petri dishes. After ~30 min attachment in the incubator, they were fixed according to the desired purpose. For tissue fixation before immunohistochemistry, tissue cultures were prefixed for 2 min at room temperature by immersion in 0.5% glutaraldehyde/4% paraformaldehyde (PA) in PBS, stored at least overnight in PA at 4°C, permeabilized with 0.1% Triton X-100 and 0.1% Tween 20 in PBS for 30 min, washed with PBS, and incubated for 10 min with a 1% solution of $NaBH_4$ to remove free carbonyl groups. For tissue fixation before enzymehistochemistry, cell cultures were treated for 2 min with PA followed by three washings in PBS.

STAINING. For immunohistochemistry, a minimum of six specimens were analyzed per study, and the conclusions drawn were representative of all samples tested. Specimens were incubated with antibody solution in PBS with 3% BSA (at 37°C for 1 h). For washing steps, PBS with 1% BSA and 0.1% Triton-X-100 was used. For double staining, primary antibodies of different species could be used together with appropriate secondary antibodies. For TF visualization, a tertiary antibody directed against the secondary antibody (both AlexaFluor 488-coupled) was necessary. Negative controls, omitting primary antibody, were made for each antibody and protocol. For

enzymehistochemistry, alkaline phosphatase (AP) activity [EC 3.1.3.1.] was visualized in briefly fixed samples (see above) after overnight incubation in the dark with continuous gentle shaking at 4°C in freshly prepared and sterilely filtered, ice-cold reaction mixture containing 3 mM naphthole ASMX-phosphate and 1 mM Fast Blue BB or 1 mM Fast Red TR (for confocal microscopic demonstration of AP) in veronal buffer pH 9.0. Dipeptidyl aminopeptidase (DAP) IV (CD 26) [EC 3.4.14.1] was visualized similarly following incubation in the mixture: 4 mg gly-pro-4-methoxy-β-naphtylamide resolved in 20 μl dimethylformamide, dissolved in 10 ml ice-cold BSS, and added to 4 mg Fast blue B . For demonstration of DiI-Ac-LDL uptake, uptake cell cultures were incubated in DMEM with 1% FCS and 10 μg/ml DiIacLDL for 5 h at 37°C. After this time, the cultures were washed and fixed.

Negative controls, omitting primary antibody, were made for each antibody and protocol.

MICROSCOPY. Specimens were inspected by bright-field, phase-contrast, and fluorescence microscopy using Dialux and Diavert microscopes (Zeiss, Göttingen, Germany). Stained preparations of single arterioles and venules were also imaged by confocal microscopy using a laser-scanning confocal fluorescence microscope (TCS NT, TCS SP2; Leica, Heidelberg, Germany). Pictures were taken with a ×40 oil objective, NA 1.4, at a resolution of ~200 nm per pixel. Dual-channel images of FITC and of rhodamine or Fast-red-TB fluorescence were recorded sequentially at 488 nm excitation/525–550 nm emission and 568 nm excitation/<590 nm emission, respectively. Z series were collected at 0.5- to 1-μm optical sections taken through the specimen. Image stacks were processed using Metamorph v. 6.1 software (Universal Imaging, Ypsilanti, MI). Brightness and contrast were enhanced as needed, and maximum intensity projections were generated for visualization.

Proteolytic disintegration of left ventricular myocardium of adult human hearts. Myocardial cells and microvessels from isolated perfused left ventricles of human donor hearts (originally intended for transplantation but rejected due to delayed transport or visible lesions) were isolated proteolytically under strictly controlled aseptic conditions as outlined in the protocol (see Fig. 2) and using the experimental approach as described in principle earlier (53). Isolated ventricles were perfused via their coronaries for 10 min at 37°C with modified, Ca^{2+}-free Ringer solution gassed continuously with carbogen. Perfusion was continued with protease solution for 30 min. Already during this digestive period, fragments of postcapillary venules were isolated online during the continuous centrifugation of the circumfused protease solution using the custom-built high-resolution cell-separation centrifuge equipped with a flow-through rotor. The centrifuge (see Fig. 3) was developed in technical cooperation with E. Bühler (Hechingen, Germany). After being sectioned with a sterile razor blade (pieces 3 × 3 mm), ~3 g of the already very smooth myocardial tissue were suspended in 20 ml Ringer solution and gently homogenized by automated pipetting. For further methodological details, see Fig. 2.

Purification of arterioles by percoll density centrifugation. Precapillary arterioles and, infrequently, also venular segments were obtained after Percoll density-gradient centrifugation of the crude preparation of microvessels in zones of the gradient with buoyant densities around 1.050 ± 0.005 or 1.058 ± 0.004 g/cm^3, respectively (Fig. 1; also see Fig. 3).

Vascular organ culture and preparation of sandwich cultures of constituent precapillary arteriolar or postcapillary venular wall cells. Isolated precapillary arteriolar segments were first cultivated for 4 days in mixed culture medium. The cultures were then incubated to confluence in human endothelial culture medium. Cell and vessel fragments of venular origin were cultivated from the beginning to confluency in mixed medium. Homogeneous cell colonies of EC or pericytes of arteriolar or venular origin were obtained from the primary cultures by scratching or incubation with dispase II solution (for details see the time-lapse video of the typical growth behavior of the two cell types in Supplemental Data; Supplemental Material for this article is available online at the *Am J Physiol Heart Circ Physiol* website; also see Fig. 7). Sandwich cultures of EC and pericytes of precapillary arteriolar (SC-PAO) or postcapillary venular origin (SC-PVO) were established using essentially the technique described by Nakagawa et al. (50). Purified EC were detached with a minimum amount of trypsin/EDTA, diluted with a 10-fold higher volume of mixed medium, seeded into Transwell inserts (specifications see *Materials*; ~10^5 cells/cm^2) and cultured under standard conditions in mixed culture medium (37°C, P_{CO_2} of 40 mmHg). One day later, small numbers of the corresponding arteriolar or venular pericytes (~10^3 cells/cm^2) were seeded onto the lower surface of the respective polyethyleneterephthalat membranes. After 4 days (analogous culture conditions), the EC had reached confluence; the inserts were then transferred to the custom-built, autoclaved filtration devices (see Fig. 8*B*) filled with prewarmed filtration medium. Before the filtration studies, the cultures were adapted for 2 days to this medium (37°C), and to seal the intercellular junctions appropriately, SC-PVO were kept under a hydrostatic holding pressure (no flow) of 2.5 cmH_2O (P_{CO_2} of 46 mmHg) and SC-PAO under 10 cmH_2O (P_{CO_2} of 40 mmHg). The subsequent filtration studies (filtration medium unchanged) were performed on such cultures under analogous conditions.

Measurement of the hydraulic conductivity L_P and the selectivity of sandwich barriers for albumin transport. Transendothelial flow through the microvascular sandwich cultures was measured continuously using an electronic balance (type: ultramicro-ME; Sartorius, Göttingen, Germany) and recorded online. The selectivity of albumin transport was measured according to Suttorp et al. (66, 67) with minor modifications. In brief: since it could not be distinguished with certainty between convection and diffusion of [^{14}C]albumin, we defined an index of transport selectivity of the sandwich cultures (SI), which was calculated every 5 min on the basis of the ^3H_2O- and [^{14}C]albumin activities in the upper and lower compartments (67). The SI against [^{14}C]albumin in the course of filtration experiments was calculated as follows: $SI = 1 - (A/B) \times (D/C)$, where A and C were the differences (in cpm/100 μl) in the [^{14}C]albumin and ^3H_2O activities, respectively, in the lower compartment of the system between times x and $x + 5$ min, multiplied by the volume of the lower compartment and B and D were the sums (cpm/100 μl) of the [^{14}C]albumin and ^3H_2O, activities respectively, in the upper compartments at the same times, divided by 2 (66). The quotient A/B reflected the albumin clearance and C/D the water clearance, whereby the latter comprised diffusive and convective parts. Practical experiments were initiated by mixing 4 ml filtration medium containing 125 nCi ^3H_2O and [^{14}C]albumin, respectively, and 1 ml 25% (wt/vol) Ficoll 70 solution (prepared with filtration medium). The radioactive solution was slowly underlayered under the filtration medium over the culture, and the measurements were started.

Statistical Analysis

All data are presented as means ± SE.

RESULTS

Distribution of AP and DAP IV in the Myocardial Microvasculature

The ecto-enzymes AP and DAP IV have long been accepted as reliable markers of myocardial capillaries and have been employed in the past to determine capillary density in animal models under various conditions (10). Figure 1 shows representative left-ventricular myocardial sections and a topographical sketch (1,200 specimens from 18 patients were investigated; results were consistent in all preparations). AP was already present in the aortic intima (Fig. 1*A*). Directly below the endothelium a second intimal cell layer could be seen,

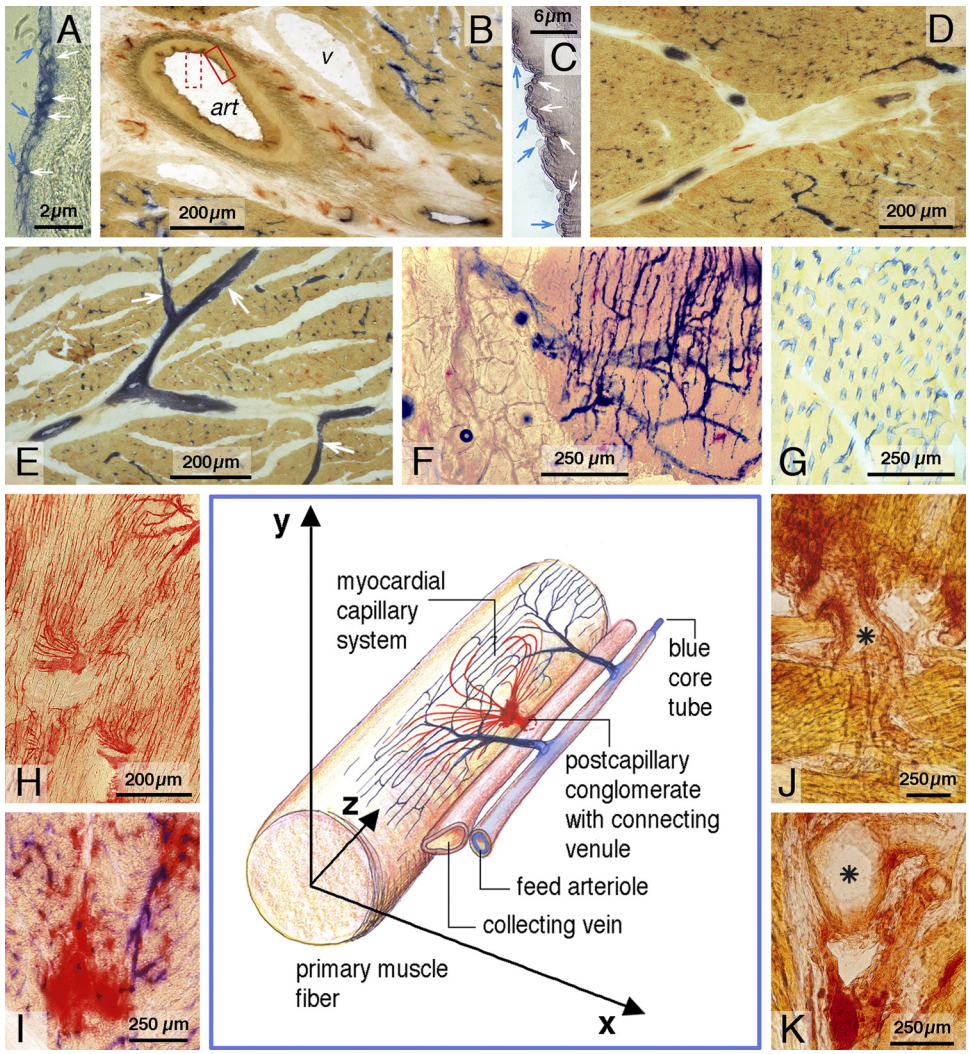

Fig. 1. Distribution of the vascular marker enzymes alkaline phosphatase (AP) and dipeptidyl aminopeptidase (DAP) IV in human left ventricular myocardium. *A*, *I*, and *K* are phase-contrast images, and all others are bright-field images. *A*: cross-section through the intima of a human aorta. Faint blue arrows indicate the luminal endothelium, and the white arrows subendothelial cells (ECs) in an AP-positive matrix (dark blue). *B*: low-power view of a connective tissue septum with a sectioned artery (art) and vein (v). Red rectangle indicates the position and orientation (dotted rectangle) of the high-power view in *C* in which the arrows are as in *A*. *D*: smaller branches of coronary arteries, multiple tangential sections revealing intimal AP (blue stain). *E*: feed arteries with branching myocardial 1st-order arterioles (arrows). *F*: arteriolar vascular tree immediately after the entry of a feed artery into actual myocardium and its downstream capillary net. *G*: cross-sectioned arterial capillaries. *H*: longitudinally sectioned, DAP-positive venous capillaries (red) and several postcapillary venular complexes; 10 μm above this plane, one of the postcapillary venular conglomerates (red) is shown in cross-section (*I*) and is now surrounded by many arterial capillaries (blue). *J*: postcapillary venular conglomerate (red) connecting with a longitudinally sectioned collecting vein (*). *K*: cross-section of a myocardial collecting vein (*) into which a partly sectioned postcapillary venular conglomerate discharges (dark red).

which expressed this enzyme on the entire circumference. Similar results could generally be documented in the intima of the larger coronary branches (Fig. 1, *B* and *C*) as well as in that of the ever smaller arteries (Fig. 1*D*) that finally approached the myocardial muscle fiber bundles as "feed arteries" in the connective tissue septa (Fig. 1*E*). AP was also detectable along all branching orders of the true myocardial arterioles (Fig. 1*F*) and further downstream with diminishing intensity to about half the length of the extensive myocardial capillary networks (Fig. 1*G*). We identified five orders of branching of these microvessels, whereby the fifth-order arterioles, representing the precapillary arterioles of the coronary vasculature, showed a continuous transition into capillaries.

The distribution of DAP was the converse of that of AP. This enzyme first appeared in the venous limb of the capillary networks, with the intensity increasing in the downstream direction (Fig. 1, *H–K*). Resembling ginger roots with their dozens of inflowing capillaries, these smallest venous collecting vessels (length: 50 ± 7 μm; $n = 25$) bend almost perpendicularly away from the plane of the inflowing capillaries (Fig. 1*H*) to connect with larger veins in which the DAP intensity disappeared rapidly (Fig. 1, *J* and *K*).

The strategic location of an AP-positive inner tube in all coronary arteries, as indicated in the sketch in Fig. 1, and the highly specific demarcation of DAP in the postcapillary venular conglomerates gave cause for extensive further consideration. As a prerequisite for more detailed histological investigations and the development of reliable in vitro models of the respective microvascular segments, we first developed methods for isolating pure preparations of the different myocardial microvessels.

Gentle Proteolytic Dissociation of Native Ventricular Myocardium to Yield Mostly Undamaged Microvascular Networks or Venular and Arteriolar Segments

The protocol shown in Fig. 2 was the result of extensive optimization studies in which a large variety of solutions, processes, and time courses were tested and compared systematically. On the basis of the technical scheme in Fig. 3, our separation procedure, although complex, is transparent and reproducible. A decisive step in the separation protocol was the purification of the microvascular segments by Percoll density gradient centrifugation (Fig. 3).

Fine Structure of Isolated Myocardial Arterioles

Classical fluorescence and bright-field microscopy studies showed that all isolated myocardial arterioles with a diameter

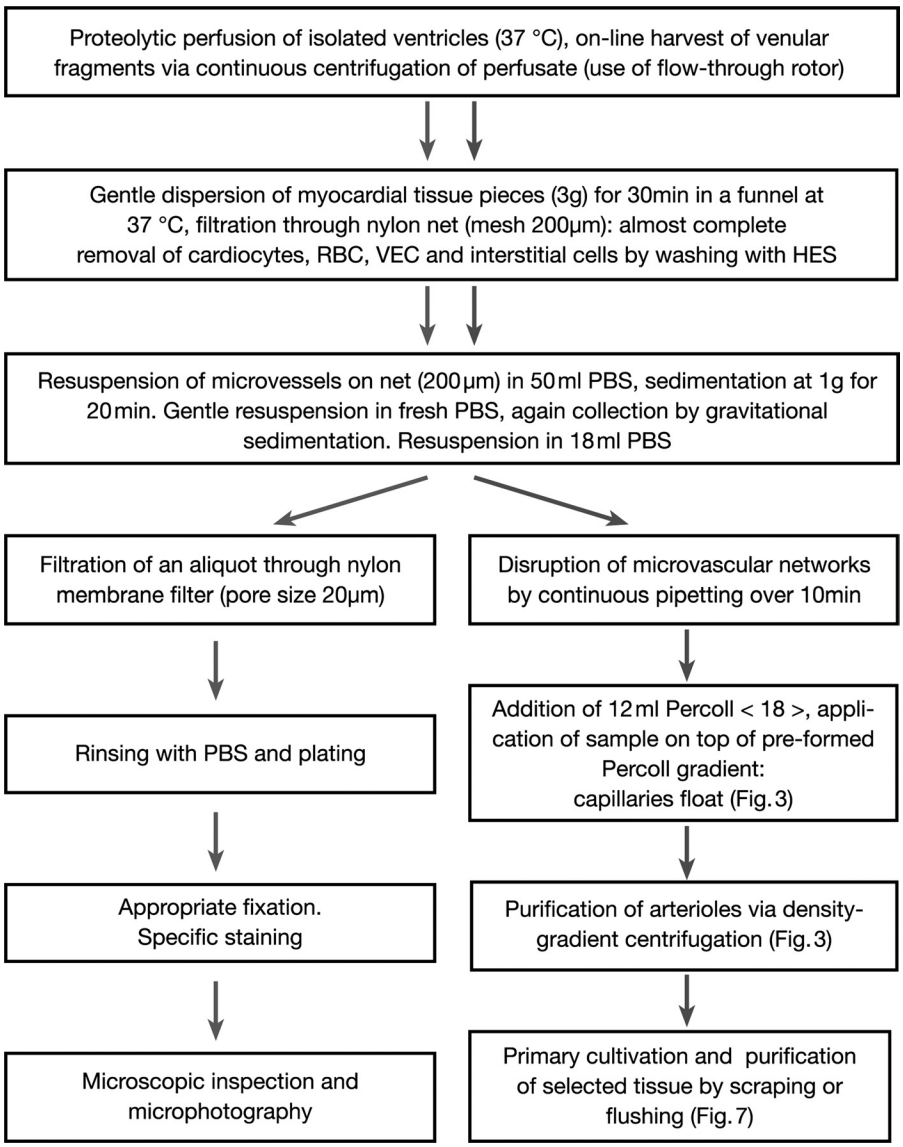

Fig. 2. Experimental protocol for harvesting and characterizing microvascular vessel segments from human myocardium. *Left* arrows indicate preparative steps for vessel isolation with optimal preservation of anatomical structure, and *right* arrows indicate the steps employed to obtain the highest possible yield for cell isolation. RBC, red blood cells; VEC, venular EC.

>20 μm were characterized by three concentric tubes (Fig. 4, *A–C*). Between the innermost endothelial tube and its adventitial envelope of SMC lied a continuous AP-positive inner tube of intermediate diameter and unexpected structure.

Confocal microscopy confirmed these observations. Preparations using enzyme-histochemical staining for AP with its red fluorescent reaction product indicated that the AP-positive tube, intermediate in the larger arterioles but the sole adventitial envelope of the endothelial tube in the precapillary arterioles, was formed by a cell type that is embedded, cocoon-like, in a continuous AP-positive ECM of interwoven filamentous and microgranular or vesicular elements. With a width of 2–4 μm, this matrix, together with its embedded cells, was remarkably thick (Fig. 4, *D–J*).

These cells that obviously produced the ECM laid very closely packed and had "antler-like" processes with which they continuously enveloped or engirded the endothelial tube, not only in the precapillary arterioles, but also in the larger (muscular) myocardial arterioles and even in the coronary arteries of all calibers in the connective tissue areas of the ventricular wall. The ECM as an essential part of the core tube of the complete arterial coronary system distinguished itself from all other myocardial structures also by the expression of the hemostasiologically important TF (Fig. 4, *K* and *L*), i.e., that membrane component that, once in contact with blood, immediately initiates coagulation processes.

AP, TF, and the presence of the cocoon-like ECM already strongly implied that the cells forming the outermost layer of the precapillary arterioles and that enveloped the endothelial core tube of all muscular myocardial arterioles and coronary arteries (forming there the intima) were not SMC. This conclusion is strengthened in Fig. 4, *M–O*. SMC encompass solely the thickest branch of the arteriolar junction in this image and, reflecting their high content of α-SMC-actin, show a far more intense (10 times higher) green fluorescence than the cells encompassing the precapillary branches. All arteriolar preparations studied using these techniques ($n = 28$) showed that the transition from muscular arteriole to precapillary arteriole was always quite abrupt, with the latter possessing no SMC at all (Fig. 4, *K–N*, and *Q*). Hereafter, we refer to former cells, which

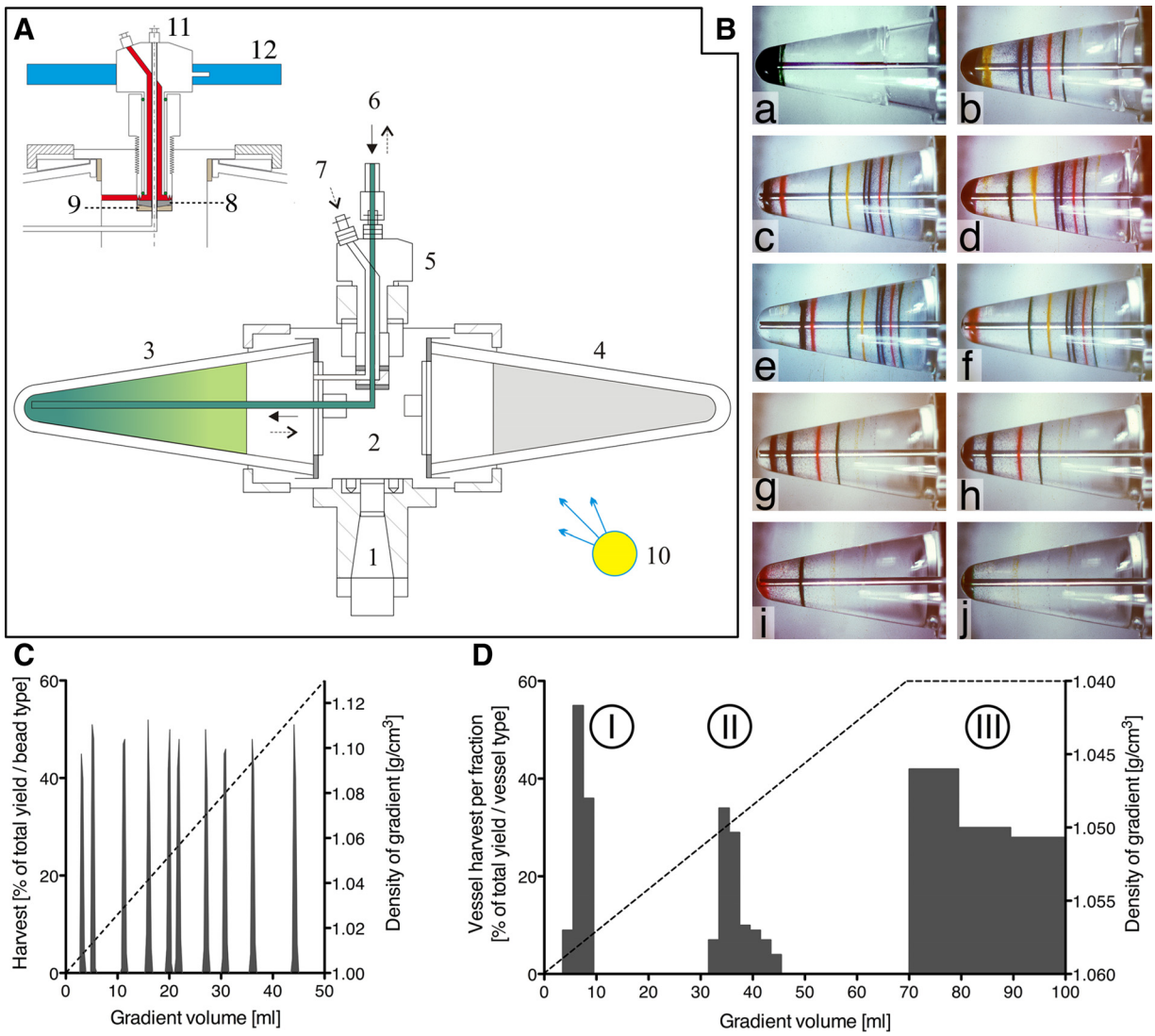

Fig. 3. High-performance density-gradient centrifugation in a custom-built centrifuge. *A*: cross-section through the rotor: *1*: rotor axle; *2*: rotor head; *3*: centrifuge glass containing a Percoll density gradient; *4*: counter-weight glass; *5*: centrally fixed tube holder; *6*: capillary tube for introducing the density gradient and for aspiration of the separated bands; *7*: tube for sample application; *10*: stroboscopic light. *Inset*: tubing holder in detail: *8*: tubing seal; *9*: steel pressure disc; *11*: lid; *12*: centrifuge cover. *B*: fractionation of colored marker beads for calibration of the Percoll density gradient, images were obtained using the light from the built-in stroboscopic lamp; *a–d*: gradual underlayering of the preformed gradient after adding a suspension of marker beads in water; *e*: sharpening of the bands by high-speed centrifugation; *f–j*: fractionation phases at low speed. *C* and *D*: graphic representation of the separation of marker beads (*left*) and vessel segments (*right*). I, venules; II, arterioles; III, capillaries and debris.

separate the endothelium and the SMC of the entire coronary arterial system, as pericytes. Although generally known as companions of capillaries in the microvascular systems of organs, pericytes have, to date, not been described in arteriolar vessels, let alone arteries. Of interest was also the observation that these cells still expressed AP in the whole arterial limb of the myocardial capillary networks (see Fig. 6*D* to compare), albeit with the intensity decreasing downstream, together with decreasing thickness of the ECM (shortly before the junction with the respective postcapillary venule between the capillary pericytes only ~100 nm).

Scanning electron microscopy (SEM) of the isolated muscular arterioles showed also that the typical pericytes entwined around the precapillary arterioles laid tightly packed and had extensively branched processes (Fig. 4, *P* and *Q*). In such preparations the partly microparticular or granular structure of the ECM could also be observed occasionally (Fig. 4*Q*). Complete proteolytic removal of the ECM revealed the extremely intimate connections between the delicate, filigree-like ends of the pericytal processes and the EC, giving the impression that the pericytes are practically "riveted" to the EC (Fig. 4*R*).

Behavior of Muscular and Precapillary Arterioles Under Tissue Culture Conditions

Muscular arterioles introduced freshly into culture (Fig. 5*Aa*) began to disintegrate already after 2–3 h, highly selectively by the initial detachment and migration of the SMC. By 12 h, these cells had completely escaped from their remaining rudimentary parental vessel and were detected in the surrounding space (Fig. 5*Ab*). Staining the culture for AP after

1 day showed the enzyme now only on the pericytes that were either compacting or spreading out on the vessel remnant (Fig. 5*Ac*). Surprisingly, there was still abundant expression of α-SMC-actin on the remnant vessel (Fig. 5*Ad*). Even after 1 day, the remnants of the endothelial tube could be recognized (Fig. 5*Ae*). The latter began to separate from the ECM and to spread out on the second day. The cellular disintegration of precapillary arterioles in culture proceeded analogously, with the exception that no SMC were present. Confocal imaging showed particularly clearly that the limiting event in the detachment and spreading of the pericytes was the degradation of the stable, AP-positive pericyte ECM (Fig. 5, *Ba* and *Bb*), in which these cells were initially virtually captured. This method also showed that the spreading pericytes immediately began again to synthesize AP-positive material, which sprouted from their plasmalemmal surface (Fig. 5, *Ca–Cc*). Freshly isolated or young pericytes budding off their parent cells therefore possessed much less AP than pericytes, which cocooned themselves completely in their ECM and thus anchored themselves to their substratum. This ecto-phosphatase was not only attached to the pericyte surface (see Fig. 8*Cd*) but also exported into the neighborhood and incorporated into microparticles, which accumulated beneath neighboring EC (see Fig. 8*Ce*). In addition to AP, the AP-positive cells of arteriolar origin expressed all the typical histological features and functions of isolated and cultured microvascular pericytes, which we characterized in extension elsewhere (50a).

EC of arteriolar origin did not express histologically detectable DAP, VE-cadherin, and α-SMC-actin, in contrast to those of venular origin (Fig. 6, *J* and *K*; Refs. 32a and 50a) but could be identified by their typical growth behavior and morphology, presence of PECAM (CD 31) and thrombomodulin (CD 141), particularly high numbers of Weibel-Palade bodies (Fig. 5*Da*), and their capacity to take up and store Ac-LDL (Fig. 5*Db*). The accompanying pericytes expressed AP constitutively (Fig. 5*Dc*), and in addition TF, ganglioside 3g5, β-receptor for platelet-derived growth-factor, connexin 43, a strongly argentophilic ECM, and high levels of α-SMC-actin, as was described in detail elsewhere (50a).

Fine Structure and Behavior of Postcapillary Venules Under Tissue Culture Conditions

In contrast to myocardial arterioles, the proteolytic separation and isolation of largely intact postcapillary venules from the myocardium were rarely successful, because venules mostly disintegrated already during the proteolytic perfusion period of the ventricular preparations. The further preparation for microscopic investigation, pipetting, centrifugation, and staining (including brief exposure to organic solvents for permeabilization), worsened the damage to these fragile microvessels. The best views of the native cell architecture of freshly isolated, vital venules, at least from the adventitial side, were thus gained by phase contrast microscopy of the vital vessels (Fig. 6*A*). These smallest venous segments in the myocardium were enveloped in contiguous pericyte tissue, the latter, however, with large intercellular gaps. The cell borders were readily recognizable, presumably by virtue of the only weak development of a stable, continuous ECM, and AP, as an ECM marker, was not detectable (Fig. 6*B*). In contrast, DAP, a specific marker enzyme for postcapillary venules in myocardial sections (see Fig. 1*B*), was also highly specific for the isolated venules (Fig. 6*B*). In all venular preparations studied ($n = 14$), the venular wall consisted of a very loose association of EC and pericytes (Fig. 6, *Ca–Cd*). SMC were never observed, nor was it possible to demonstrate the presence of AP in venules, in contrast to its presence in arterioles and in the arterial limb of the capillary networks (Fig. 6*D*). This again implied that venules lack the thick, interwoven ECM of the arterioles and arterial capillaries. After seeding of venular fragments in tissue culture (Fig. 6*E*), it became clear that not only the EC but also the pericytes in the venular wall initially expressed high DAP activity. The pericytes soon (2–8 h) migrated from the wall of the initial vessel and spread out around the degenerating endothelial tube (which was usually still recognizable, Fig. 6*E*). These cells also expressed TF and α-SMC-actin (not shown). SEM gave greater insight into the morphology of venular decomposition in tissue culture (Fig. 6*F*). It became clear, for instance that from the beginning the EC established central colonies with the typical "paving-stone" architecture (see also video in Supplemental Data). The accompanying pericytes consistently surrounded the EC but now, no longer in direct contact with the latter, rapidly changed their phenotype to that of arterial pericytes and again expressed AP (Fig. 6, *G* and *H*). The presence of pericytes, with their "nursing" (50a), accelerated venular endothelial growth in these proliferating cultures remarkably (cell doubling time in presence of pericytes only 11 ± 1.5 h, $n = 8$; in their absence 16 ± 2.1 h; $n = 8$). Cultured EC of venular origin incorporated acetylated LDL (not shown) and expressed general endothelial markers, such as von Willebrand factor antigen (Fig. 6*J*), and markers typical of endothelium involved in immunological recruitment processes, such as abundant DAP (Fig. 6, *G* and *I*), PECAM-1 (Fig. 6*J*), ICAM-1 (not shown), and VE-cadherin (Fig. 6*K*). In contrast to arteriolar endothelium that stored von Willebrand factor antigen in far more abundant Weibel-Palade bodies (Figs. 4*O* and 5*Da*), the expression of this protein in the cultured venular endothelium was weak (longer exposure times necessary) and diffuse, and Weibel Palade bodies existed only in direct vicinity of the nuclei (Fig. 6*J*). In addition, EC of postcapillary venular origin expressed unusually high concentrations of α-SMC actin, although the concentration of this contractile protein was approximately times higher in pericytes and seven times higher again in SMC (50a).

Homogenous Preparations of EC and Pericytes from Organ Cultures of Purified Precapillary Arterioles and Postcapillary Venules

Organ cultures, established from the peak maximum of the vessel yield I and II after Percoll density gradient centrifugation (Fig. 3), were the starting point for the purification of the different vascular cells. The organ cultures were inspected microscopically in the first days after seeding and, if necessary, purified further using sterile spatulas. From one human heart, we were able to establish 100–200 cultures of each vessel type in standard 35-mm Petri dishes. The subsequent characteristic and spontaneous segregation of pericytes and EC of venular

origin (Fig. 6, *G* and *H*) in culture was due to the vigorous growth of the former, displacing the latter (see Fig. 7, *Aa–Ad*; also see time-lapse film in Supplemental Data), and allowed the successful establishment of pure cultures of both cell types. After extensive areas of EC colonies (>5 mm diameter) had formed, these could be separated simply from their pericyte fringe using sterile spatulas under microscopic observation (Fig. 7, *Ba–Bc*) and the detached pericytes reseeded. A more convenient method than the time-consuming mechanical separation, comprised incubation of the mixed culture at 37°C for 30 min in a 0.1% dispase II solution (Fig. 7, *Ca–Cd*). After either of these procedures, the pericytes, now only weakly adhering, could be removed using syringes or pipettes or, most reproducibly, with a custom-built rinsing apparatus (technical

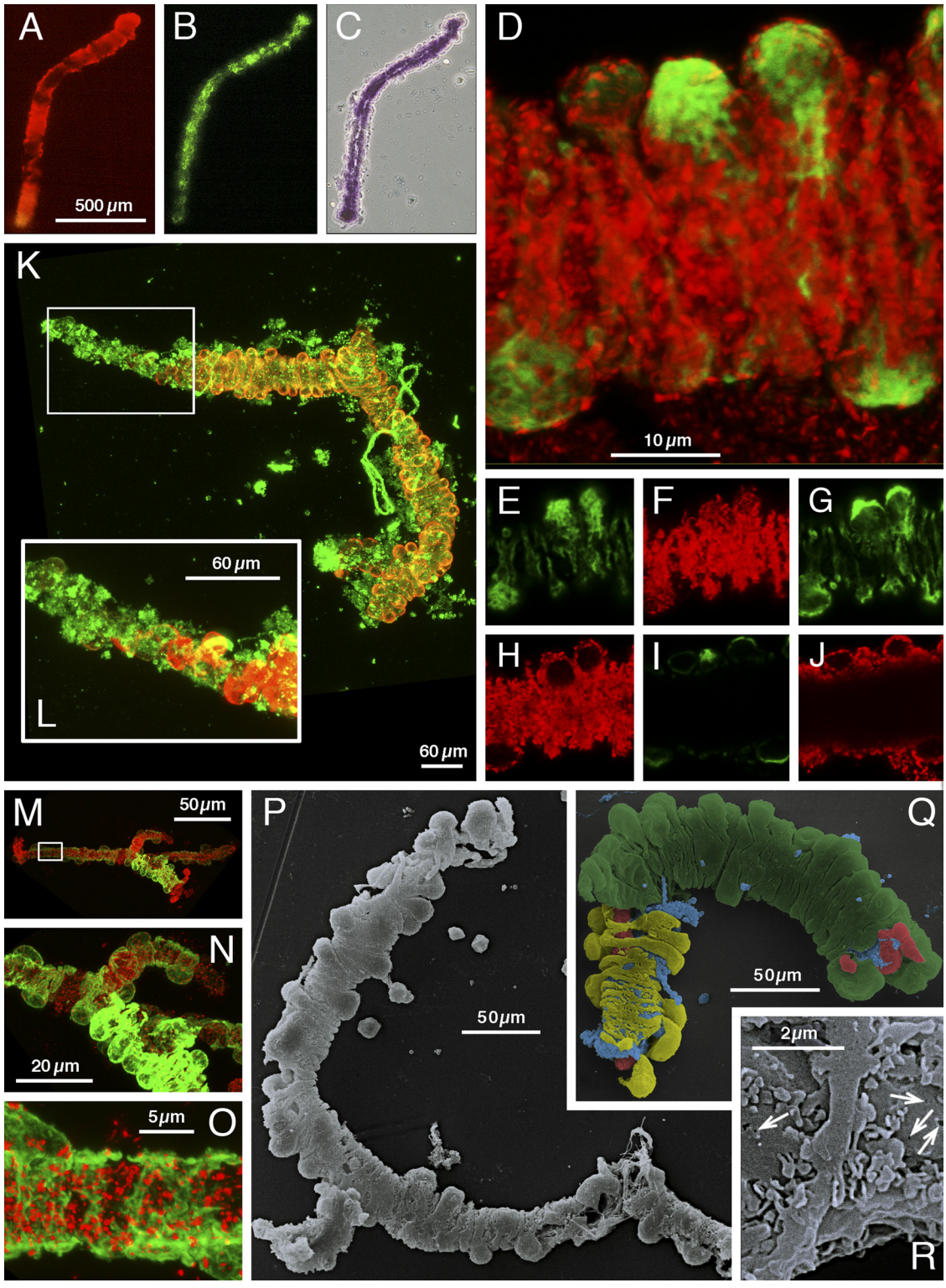

details are shown in Fig. 7*D*) and subsequently reseeded and grown in highly pure cultures [see also (50a)].

Model for the Measurement of Diverse Barrier Functions of Microvascular Vessel Walls Reconstructed In Vitro

Figure 8 shows major histological characteristics of the SC-PAO or SC-PVO established on Transwell insets, as well as the technical features of the custom made filtration system The upper panel within the red frame (Fig. 8*Aa*) is a transmission electron micrograph of a cross-sectioned vascular EC monolayer, showing the extent and the considerable degree of organisation of the normally closed, overlapping clefts (endpoints marked by black arrows) of venular endothelium. The SEM pictures below show the continuous cellular barrier of such a confluent cell sheet. The clefts appear as zipper-like structures (white arrows in the *inset*). The loose network of pericytes (Fig. 8*Ab*, green frame) on the lower surface of the filter leaves large areas of the filter uncovered (black arrows) and thus seems likely to have little, if any, influence on the L_P of the SC-PVO (measurements subsequently confirmed this conjecture, see below). In contrast, pericytes of arteriolar origin in contact with their appropriate endothelial culture (SC-PAO) enveloped themselves increasingly in a thick ECM that contributed significantly to the barrier behavior of the SC-PAO (and their contours could no longer be seen in SEM pictures). Using well established methods (31), we were able to show that within the period of our standardized cultivation procedure only 0.5 ± 0.2% (12 cultures from 12 donors) of the filter pores were occupied by cellular processes from EC and/or pericytes.

The technical details of the custom-built apparatus for measuring hydraulic conductivity are shown in Fig. 8*B*.

The presence or lack of an ECM could already be demonstrated macroscopically after staining sandwich cultures for AP and DAP (Fig. 8, *Ca–Cc*). Figure 8*Ca* shows the unspecific yellow color of a SC-PVO after negative staining for AP, but additional staining of such preparations for DAP showed the intense red product of DAP at the surface of the venular endothelial cells (EC; Fig. 8*Cb*), as was seen characteristically also in appropriately stained venules either in situ in the myocardium or freshly isolated. In contrast, analogous double staining of SC-PAO yielded the intense blue color (Fig. 8*Cc*), which, as described above, is characteristic of AP and a well-developed arteriolar ECM (and the arteriolar EC were not stained red due to the lack of DAP). Inspection of high-power phase-contrast micrographs of analogous mixed cultures stained for AP focused in the plane of the pericytes (Fig. 8*Cd*) or in that of the EC above them (Fig. 8*Ce*) showed masses of AP-positive (blue) ECM material in microparticular form emanating from the pericytes both in their immediate vicinity and as a deposit directly below the EC. These sandwich cultures of arteriolar origin were characterized by a lower L_P and distinctly higher selectivity values for albumin than those of venular origin (see Fig. 9).

Measurement of L_P and SI for Albumin Transport in Different SC-PVO and SC-PAO

As shown in Fig. 9, the L_P of control SC-PVO cultures in a human plasma-like medium (filtration medium) was substantially lower ($2.6 \pm 0.3 \cdot 10^{-7} cm \cdot s^{-1} \cdot cmH_2O^{-1}$; $n = 10$) than that of cultures incubated in standard culture medium (DMEM containing 10% v/v FCS; $1.4 \pm 0.1 \cdot 10^{-6} cm \cdot s^{-1} \cdot cmH_2O^{-1}$; $n = 10$). Simultaneously, the SI for the transmural movement of albumin fell from 0.9 ± 0.03 to 0.5 ± 0.04 ($n = 10$ in each case). In contrast, the mean L_P of SC-PAO in plasma-like medium ($L_P = 3{,}2 \pm 0{,}5 \cdot 10^{-8} cm \cdot s^{-1} \cdot cmH_2O^{-1}$; $n = 37$) was only about one-tenth of that for SC-PVO, nor did it increase on exposure to serum-containing medium. In addition, the SC-PAO barrier was almost impenetrable for albumin (SI: 0.9 ± 0.02; $n = 30$) under all conditions.

The L_P of filter cultures with a confluent venular EC layer ($1.2 \pm 0.2 \cdot 10^{-6} cm \cdot s^{-1} \cdot cmH_2O^{-1}$; $n = 8$) was substantially higher than that of cultures of these EC in contact with their pericytes ($2.6 \pm 0.3 \cdot 10^{-7} cm \cdot s^{-1} \cdot cmH_2O^{-1}$, $n = 8$), while that of similar filters carrying solely a venular pericyte layer was ~100 times higher. SC-PAO behaved quite differently. The L_P and SI of arteriolar confluent endothelial monolayers alone ($8.4 \pm 1.3 \cdot 10^{-8} cm \cdot s^{-1} \cdot cmH_2O^{-1}$; 0.84; $n = 8$) were higher than those of the cocultures ($3.2 \pm 0.5 \cdot 10^{-8} cm \cdot s^{-1} \cdot cmH_2O^{-1}$; 0.95), and filters carrying solely 3-wk-old cultures of pericytes with their well-developed ECM (see Fig. 8*Cc*) were quite tight (L_P: $2.6 \pm 0.6 \cdot 10^{-7} cm \cdot s^{-1} \cdot cmH_2O^{-1}$; SI: 0.9; $n = 10$).

DISCUSSION

Enzyme-Histochemical Identification of Human Left Ventricular Arterioles and Venules

AP is a very typical marker enzyme for the entire arterial side of the coronary system. A conspicuous finding, made

Fig. 4. Wall structure of precapillary and muscular arterioles isolated from human left ventricular myocardium. *A–C*: fluorescence micrographs of a muscular arteriole after staining for α-smooth muscle cell (α-SMC)-actin (red), von Willebrand factor (vWF; green), and AP (blue). *D*: precapillary arteriole after immune-histochemical staining for α-SMC-actin (green) and enzyme-histochemical staining for AP (red). Image is a maximal intensity projection obtained by confocal microscopy after scanning 30 layers each 1.0 μm apart. *E–J*: scanned images in planes demonstrating the extracellular matrix (ECM) cocoon, from the outermost part of the upper surface of the vessel (*E* and *F*), 6 μm deeper (*G* and *H*), and a further 9 μm deeper (*I* and *J*) in the midline of the vessel course. *K*: transition from a muscular arteriole to a precapillary arteriole (frame). SMC of the former are stained for α-SMC-actin (red). Pericyte sheath (see enlargement in *L*) in the abruptly beginning precapillary arteriole is stained for TF (green). *M–O*: segment of a muscular arteriole with its precapillary arteriolar branches. Weibel-Palade bodies in the endothelial tube fluoresce red, and the intense green fluorescence indicates α-SMC-actin in the smooth muscle cells, the weak green fluorescence indicates the pericyte layer. *P* and *Q*: scanning electron microscopy (SEM) of a precapillary arteriole and a muscular arteriole, respectively. *Q*: typical abrupt transition to the precapillary extension of a small muscular arteriole. The latter is practically the continuation of the muscular arteriole's double-layered-EC and pericyte-inner tube. Partial proteolytic dissociation of this emerging vessel segment loosened the cellular components such that the shear forces resulting from arteriolar fixation pulled these apart, revealing informative structural details (which are not apparent in the intact precapillary arteriole in *P*). For clarity, the recognizable mural structures in *Q* are underlayed with colors: SMC, green; pericytes, yellow; residual granular oder fibrillar components of the ECM (which originally enveloped the pericytes completely), blue; central endothelial tube, red. *R*: higher magnification showing the connection between a precapillary arteriolar pericyte and the underlying endothelium. White arrows indicate tiny holes in the endothelial surface where terminal processes of the pericyte were broken off in the course of preparation.

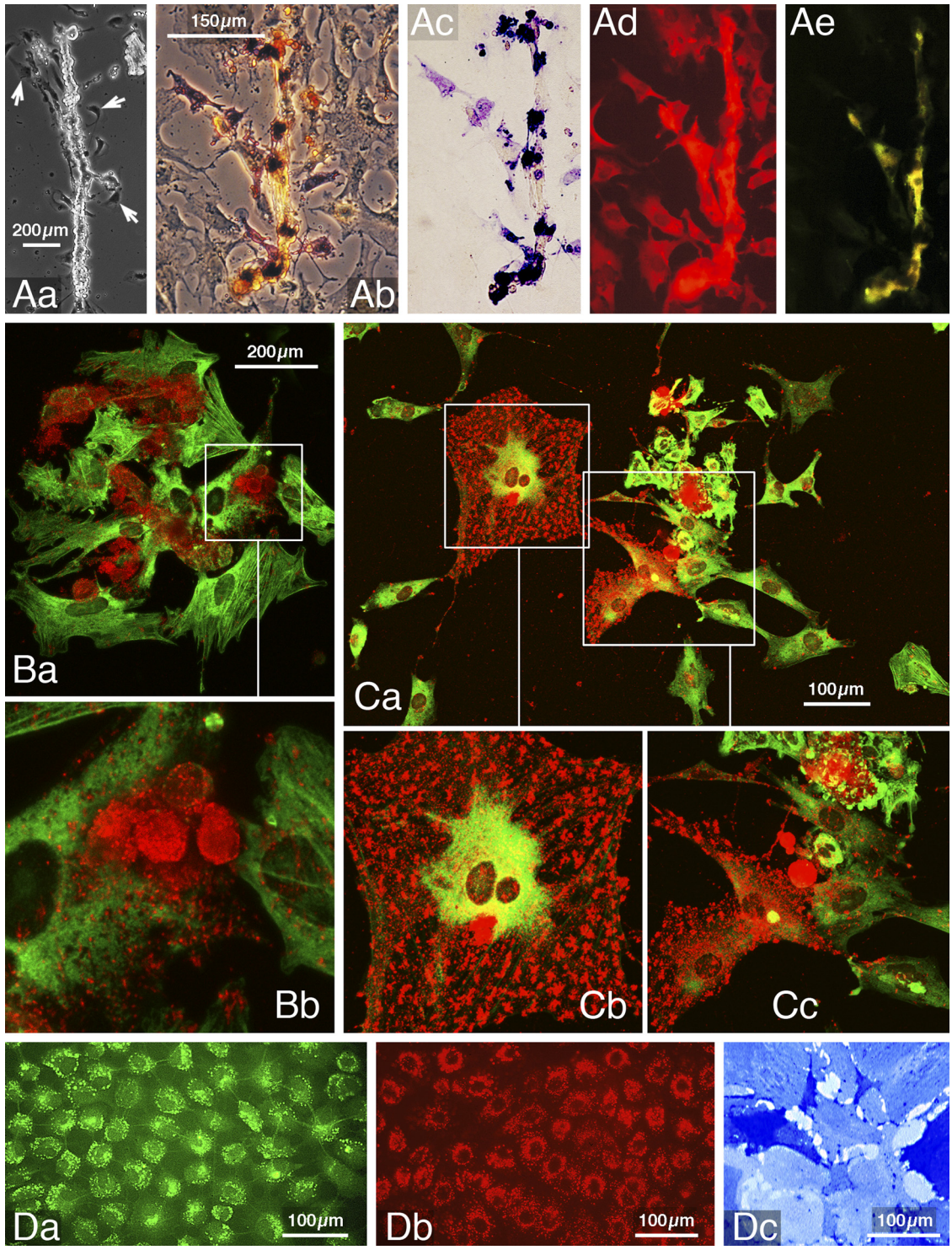

Fig. 5. Arterioles in organ culture. *A*: a larger, muscular myocardial arteriole in culture. *Aa*: phase-contrast image 3 h after seeding. Arrows point to spreading SMC. *Ab*: phase-contrast image 12 h later. *Ac*: bright-field image 36 h later, double staining for AP (blue) and DAP (faint orange). *Ad* and *Ae*: Fluorescence micrographs of the preparation shown in *Ac* after staining for α-SMC-actin (red) and vWf (green), respectively. *B*: confocal images of fragments of a muscular arteriole in culture. *Ba*: enzyme- and immune-histochemical staining for AP (red fluorescent precipitate) and α-SMC-actin (green fluorescence) respectively 15 h after seeding. All the SMC have spread out. *Bb*: Enlargement of the inset in *Ba*, showing the round, compacted form of the contracted pericytes still enveloped by their dense ECM (red). *Ca*: similar culture after 36 h, stained for AP (red) and vWF (green). *Cb* and *Cc*: enlargements of the respective *insets* in *Ca*. Pericytes are now in the process of spreading out and organize the formation of new ECM on their surface (red precipitate); the ECs will follow and subsequently form colonies 1 day later. *Da* and *Db*: identification and characterization of ECs of arteriolar origin in pure culture by their particularly strong expression of vWF (green) and uptake and storage of Ac-LDL (red) respectively. *Dc*: pure culture of pericytes, stained for AP (bright-field image) (for further histological characterization, see Ref. 50a).

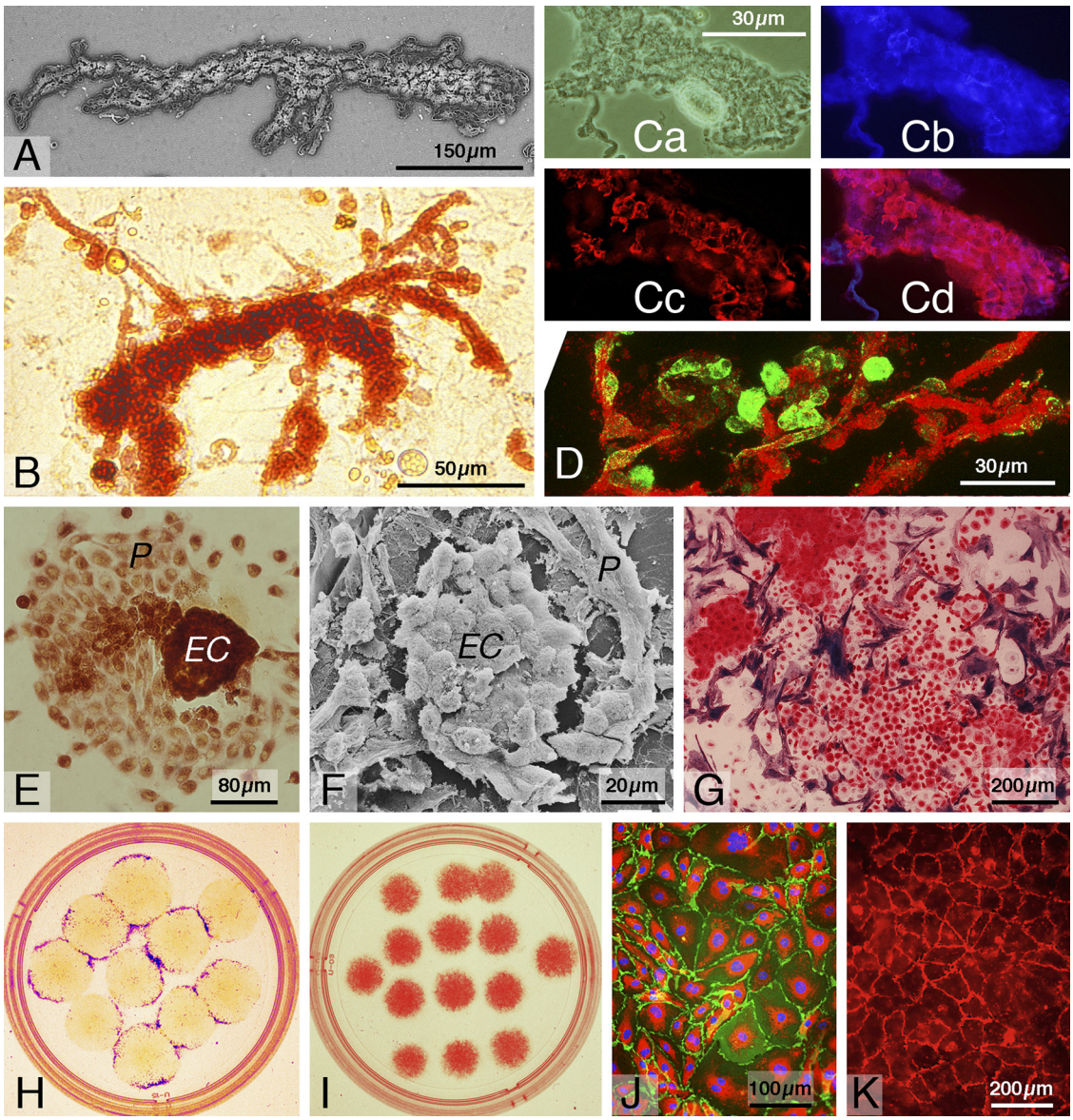

Fig. 6. Histological properties of postcapillary venules immediately after isolation and during culture. *A*: phase-contrast image of a vital venule. *B*: branched venule with attached capillaries, DAP-positive, AP-negative. *C*: wall tissues of an isolated postcapillary venule. *Ca* phase-contrast. *Cb* and *Cc*: confocal images after staining the endothelial lining for vWF (blue) or the pericytes for α-SMC-actin (red). *Cd*: double exposure. *D*: confocal image (maximal intensity projection) of isolated arterial capillaries stained immune-histochemically for α-SMC-actin (green) in pericytes and enzyme-histochemically for AP incorporated in the ECM (red). Innumerable red-stained microparticles are evidence for the granular structure and the partial proteolytic degradation of the pericyte ECM, which otherwise completely envelops capillaries in the arterial limb of the myocardial microcirculation. *E*: postcapillary venule 8 h after seeding in tissue culture, bright-field image after staining for DAP; EC clumped ECs from the former core tube. P, pericytes. *F*: SEM of a specimen analogous to *E*. *G*: mixed culture of venular ECs (staining for DAP) and pericytes (blue staining for AP) after 1 wk in culture. *H*: colonies derived from a highly red purified venular preparation 2 wk after seeding in multiple circular spots (3–4 mm diameter) in a 6-cm diameter Petri dish. Contaminating pericytes (blue) surround the endothelial colonies (faint orange). *I*: fully differentiated, spot-like colonies of purified venular ECs (red staining for DAP). *J*: immunofluorescent staining of homogenous confluent cultures of ECs of venular origin for platelet EC adhesion molecule (green), vWF (red), and nuclei (blue). *K*: as in *J*, staining for VE-cadherin.

initially in the larger and smaller arteries, was that AP was not expressed in the media but selectively in the subendothelial cell layer of the arterial intima. This was of particular interest in view of our recent finding of a subendothelial cell population (subsequently identified as pericytes) constitutively present in the intima of human aorta and healthy large human veins (32). There, however, AP was expressed only when endothelial damage exposed these cells to serum. Thus, in contrast to the arteries of the coronary system, AP in large vessels of the systemic circulation serves as a marker for pericyte activation in the intima. In the coronary system, the constitutive myocardial arterial AP activity extended downstream into the arterial limb of the capillary bed, albeit diminishing rapidly and being absent in the venous limb of the capillary bed. Conversely, DAP activity began to appear in this region, increased rapidly downstream to a maximum in the bizarre, root-like form of the postcapillary venular complexes, and subsequently disappeared again after the transition to the next order of veins. In

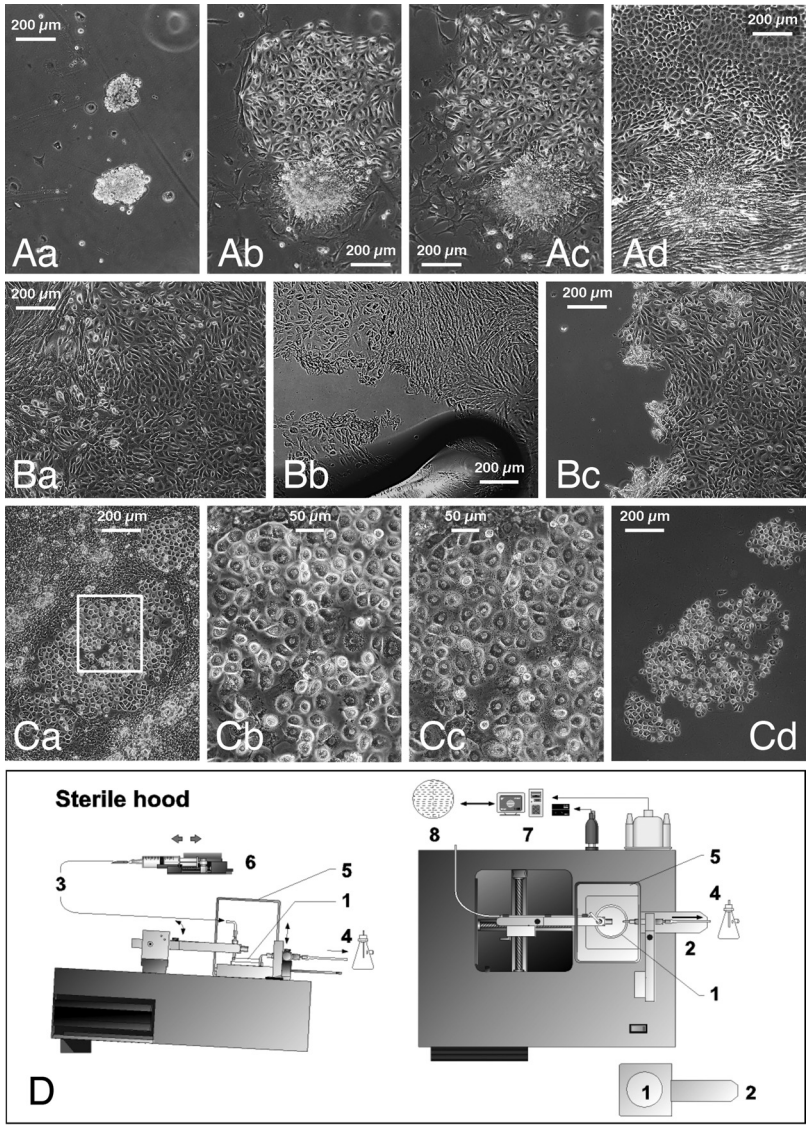

Fig. 7. Purification of cultured ECs and pericytes of arteriolar or postcapillary origin. *A*: clump of ECs and of pericytes, both of arteriolar origin, 1 h after seeding (*Aa*), and 24 h (*Ab*), 32 h (*Ac*), and 90 h later. *B*: purification of selected vascular cell colonies with a sterile glass spatula under microscopic control. Start of the procedure for purifying an endothelial colony of postcapillary origin (*Ba*), use of the spatula (*Bb*), and purified central endothelial colony (*Bc*). *C*: larger numbers of endothelial cultures of postcapillary origin could be purified specifically by incubation in an appropriately adjusted solution of dispase II (10% wt/v) in Ca^{2+}-free HEPES-buffered Earle's salt solution (HES) at 37°C. *Ca*: starting situation. *Cb*: after the incubation (1 h) in protease solution. *Cc*: culture after 90 min recovery in culture medium at 37°C, both enlargements of the frame in *Ca*. *Cd*: culture (same magnification as in *Ca*) after selectively rinsing off the loosely anchored or detached pericytes by use of the automatic custom-built rinsing system shown in *D*. *D*: *1*: primary mixed culture in holder (*2*); holders for inflow (*3*; rinsing solution HES) and aspiration (*4*) cannulae (inner Ø 0.8 mm); *5*: transparent, autoclavable hood; and *6*: infusion pump adjusted to a flow rate of 45 ml/min. Position of the inflow tube holder was controlled by a computer 7 running custom-written software that generated a meandering movement 8 of the inflow cannula across the bottom of the culture dish, thus rinsing the entire culture uniformly with optimized shear forces.

the myocardium, therefore, DAP is a marker for vessel conglomerates formed by the venous capillaries and postcapillary venules, i.e., that part of the microvasculature that is specialized for recruitment of the immune defense (1, 25, 56). The schematic topography of the coronary microvascular architecture proposed in Fig. 1 is remarkably consistent with the far earlier studies of Brown (8) using Indian Ink injections. Brown also described the conspicuous postcapillary venule complexes ("turnip root venules") for the first time, which have not been described in any other organ as yet. Each of these venules was already a collecting vessel into which (up to) dozens of capillaries discharged. Our studies showed clearly that the plane of sectioning had a decisive effect on the vessel type seen in the section (arterioles and their downstream capillaries, or venous capillaries and their post capillary venules). This is certainly a major reason for the frequently reported discrepancies in studies using double staining for AP and DAP to assess capillary density (10).

Our findings are also consistent with the optical sectioning studies of Kassab's et al. (33, 35–37) on elastomere casts of the porcine coronary system, and indeed our cell-biological studies at the microcirculatory level extend the latter.

Descriptions of myocardial microvascular architecture based on corrosion casts and evaluated using SEM (2) also concur well with our findings. In particular, we could confirm that the diameter of genuine myocardial arterioles is in the range 8–100 μm, and the mean diameter of all arterioles measured in the present histological study (18 ± 3 μm; $n = 162$) was close to the 16.5 μm measured for the canine heart (2). In our experience, in human ventricular tissue, there is always an abrupt transition from the larger, upstream myocardial arterioles with their smooth muscle layer (muscular arterioles) to nonmuscular, terminal arterioles at a diameter of ~20 μm. The lower mean diameter (18 μm) of the continuum of myocardial arterioles strongly implies that these pericyte-engirded (see below) resistance vessels constitute the majority of all myocardial arterioles (see also Refs. 21, 28, 53).

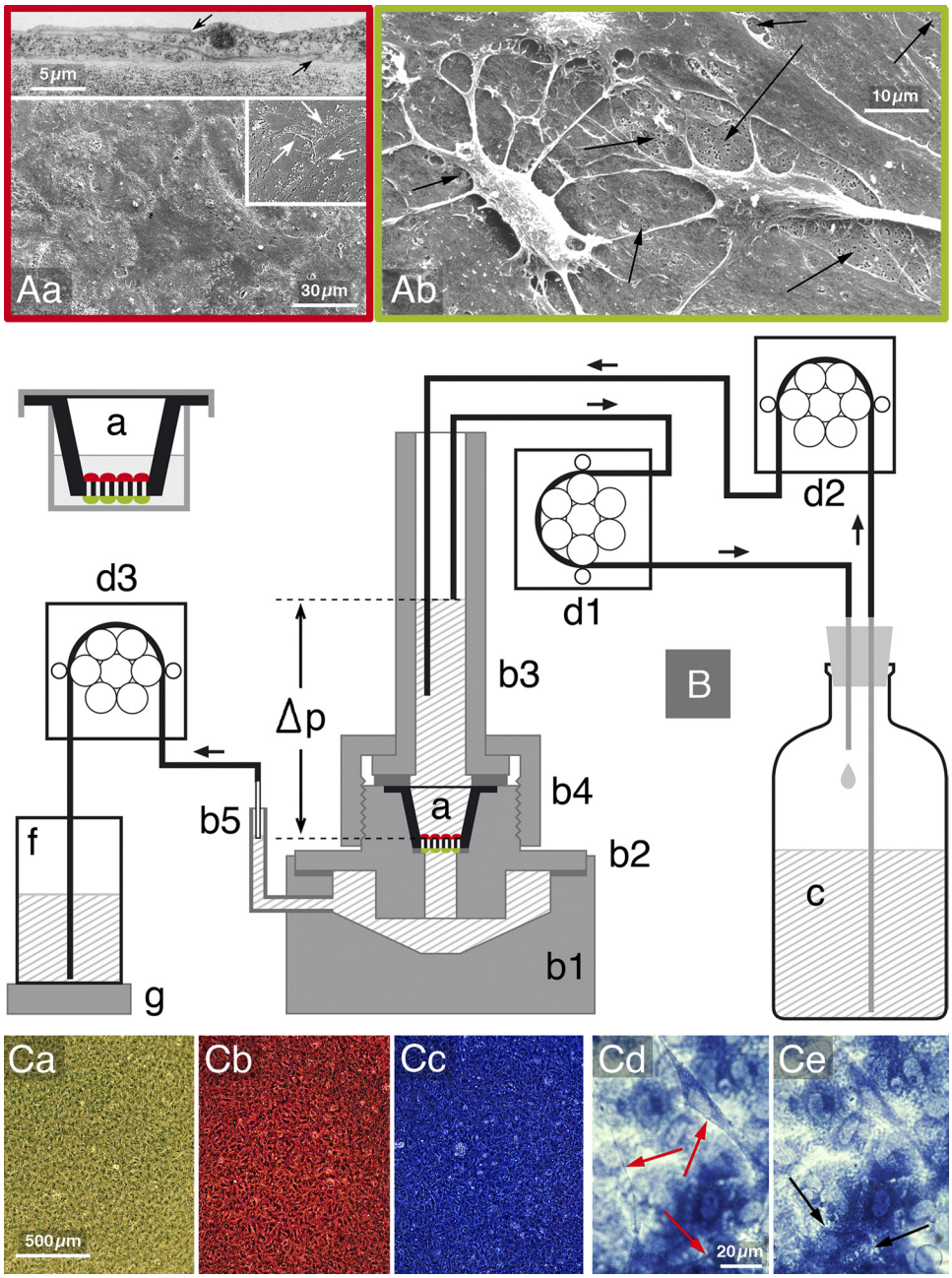

Fig. 8. Histological features of sandwich cultures of ECs and pericytes of postcapillary venular or precapillary arteriolar origin [precapillary arteriolar (SC-PAO) and postcapillary venular origin (SC-PVO), respectively]. *Aa* (red frame) and *Ab* (green frame): surface morphology of a confluent endothelial sheet of SC-PVO on top of a porous filter and a loose net of the appropriate pericytes on the lower filter surface, respectively. *Aa*, *top*: cross-section through 2 adjacent EC on top of the filter (transmission electron micrograph). *B*: custom-built apparatus for measuring hydraulic conductivity of sandwich cultures. *a*: Transwell chamber. *b*: disposable chamber system (parts *b1–b5*); its rise tube (*b3*) was filled with the fluid to be filtered from a reservoir (*c*). Hydrostatic pressure head to which the tissue layer was exposed was set (and maintained) by adjusting the pump rates of the outflow (*d1*) and inflow (*d2*) pumps. Filtrate was rinsed in a narrow outlet tube (*b5*) from which it was aspirated continuously via a fine steel capillary tube attached to a roller pump (*d3*). *f*: Water-filled beaker standing on a sensitive electronic microbalance, which, online-connected with a computer system (not shown) allowed the rate of filtration to be calculated and registered. *C*: enzymehistochemical stainings of various sandwich cultures. *Ca*: SC-PVO, negative staining for AP. *Cb*: as in *Ba* after positive staining for DAP. *Cc*: SC-PAO after staining for both enzymes but only the staining for AP was positive. *Cd* and *Ce*: high power phase-contrast micrographs of cocultures of ECs and pericytes after staining for AP focused in the plane of the pericytes (*Cd*; red arrows point to fine cell processes) or the ECs (*Ce*; black arrows).

Isolation and Purification of Precapillary Arteriolar and Postcapillary Venular Vessel Segments

The ventricular myocardium is a firm and richly vascularized tissue. Besides the mass of cardiocytes and the cells of the vascular and lymphatic systems, there are numerous other cell types such as fibroblasts, mast cells, macrophages, and interstitial cells of unknown function. In view of this cellular diversity, the ambitious goal of the present study, establishment of pure cultures of endarteriolar and postcapillary venular cell types, could only be approached by developing a strategy and protocol for first isolating the relevant microvascular vessel segments after gentle proteolytic disintegration of myocardial tissue, the principal experimental approach of which has been developed earlier (53). A particularly important prerequisite in the experimental protocol was the commercial availability of reliable and strictly standardized collagenase and dispase preparations that guaranteed complete tissue disintegration while ensuring that the vessel segments retained their typical differences in specific density. These differences were very small but nonetheless adequate for tissue separation. Our custom-built cell separation centrifuge (Fig. 3) combined high-performance centrifugation with an unusually high separative efficacy. The main reason for this was that the formation as well as the fractionation of the density gradients was performed during continuous centrifugation, thus avoiding turbulence artifacts. Myocardial components separated using this method could also be purified effectively from possible microbial contaminants. The modification of the rotor for through-

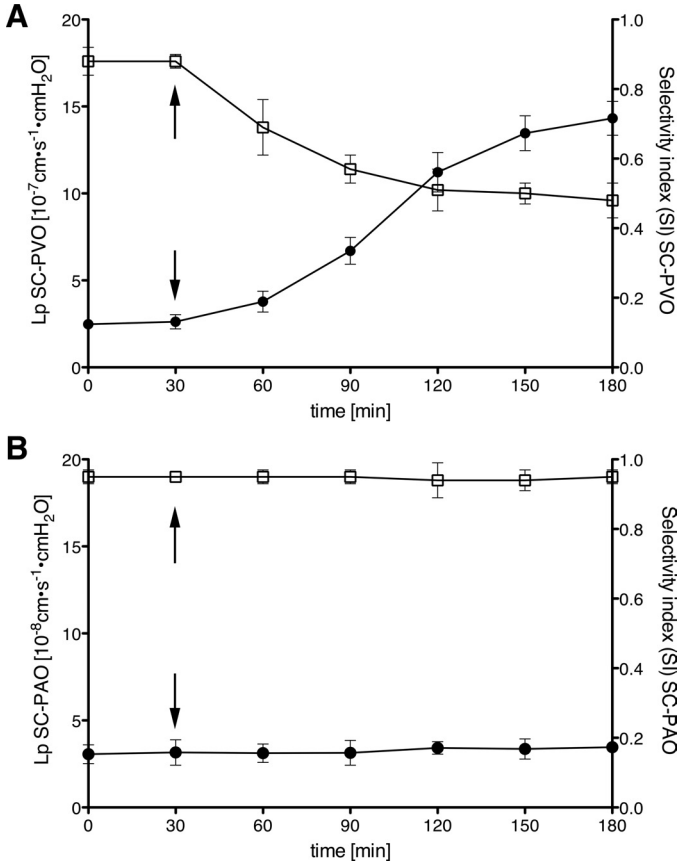

Fig. 9. Basic characterization of the barrier behavior of SC-PVO and SC-PAO by measurement of the hydraulic conductivity (L_P) and the selectivity index (SI) for transmural passage of albumin. *A*: time course of L_P (points) and SI (□) for SC-PVO during initial incubation in plasma-like medium, and after changing the medium (arrow) to serum-containing medium. *B*: as in *A* but for SC-PAO.

flow operation allowed the prompt and very selective isolation of fragments and cells of postcapillary venular origin already during the proteolytic perfusion of the hearts. The methodological experience gained enabled the subsequent development of technically simpler separation protocols employing standard centrifugation techniques (50a).

Detection of Pericytes and Their Peculiar ECM as a Constituent Barrier Within the Wall of all Myocardial Arterioles

Both high-resolution confocal microscopy and SEM showed that the precapillary arterioles were consistently engirded with a single layer of cells that are completely enveloped, cocoon-like, in their ECM, the latter expressing uniformly high levels of the ecto-enzyme AP. This embracing matrix has long been regarded as very characteristic peculiarity of microvascular pericytes (74), although current opinion still holds these cells to be restricted to the capillary system and the venules (13, 14, 65, 78). Further evidence that the AP-producing and -exporting cells were not SMC came from investigations on their actin content, which was only one-seventh that of the accompanying SMC. After their successful isolation and cultivation, we have identified these cells in more histological detail and also functionally as genuine pericytes [see separate study (50a)].

In addition to the cell membrane of the pericytes, AP was also present in high concentrations in microparticular or microvesicular structures of the ECM, just resolvable with light microscopy (see Fig. 8, *Cd* and *Ce*, and Ref. 50a), deposited on the abluminal surface of cocultured EC, leading to the recurring, but erroneous, belief that AP is an endothelial marker (20, 43, 57). In this respect, the arteriolar pericytes resembled those in the subendothelium of the aorta and of large human veins after their activation (32). Membrane-bound enzymes such as AP may be released from cells in forms that retain the lipid components that mediate their anchorage within membranes. Hydrophobic isoforms of membrane-bound enzymes are also able to undergo postrelease aggregation, both with themselves and also with other hydrophobic molecules (48). Thus exported AP aggregates could confer a substantial degree of hydrophobicity on the pericyte-derived ECM layer enveloping the endothelial tube. Consistent with this view is the high affinity of the ECM for the lipophilic azo dye enzyme-histochemically formed to demonstrate AP activity. Not even organic solvents such as ethanol or acetonitrile were able to wash the dye out of the preparations. The putative lipid content, and hence lower specific density, of the ECM may also explain the successful separation of the lighter arterioles from the remarkably heavier venules (ECM largely absent) by density-gradient centrifugation. The even lower specific density of the capillaries may be accounted for by their very high proportion of cell membrane (see Fig. 3*D*).

The above considerations are of considerable functional relevance, since the filamentous, and at the same time microparticulate, ECM appeared, at least in confocal images, as a particularly dense barrier that contributed substantially to separation of the endothelial tubes from the extravascular space of precapillary arterioles. Indeed, the pericyte layer with its ECM cocoon around the inner endothelial tube was also consistently apparent in the muscular arterioles. Its presence may explain the old paradoxical observation that a whole group of hydrophilic substances act as vasoconstrictors in direct contact with the vascular smooth cells of an artery but are potent vasodilators when present intravascularly. Such vasoactive compounds can induce a rapid release of nitric oxide from the arteriolar endothelium (6). This small, lipophilic, and therefore extremely rapidly diffusible, molecule can obviously reach the contractile cells of the resistance vessels promptly, and there mediate the originally unexpected and strong vasodilator effect of the triggering compounds ("paradox effects of vasoactive substances like acetylcholine"; Ref. 16).

The finding that the great majority of the arterioles in human myocardium that play the key role in the control of myocardial vascular resistance (i.e., those with diameters <20 μm) have no SMC, but rather a pericyte coat, sheds new light on hitherto accepted models of blood flow regulation and relevant pharmacological reaction mechanisms. One fact appears to be clear: the role of the pericytes in the control of blood flow, while repeatedly suggested (15, 34, 39, 40), has been greatly underestimated. It must be assumed that the tension of the SMC of the muscular arterioles is controlled by mechanisms very different from those controlling the pericyte/ECM barrier that separates the former from the endothelial tube and forms the sole contractile tissue of the terminal and most important resistance vessels. Numerous studies in arterioles in situ (e.g., Ref. 14), as well as our own in vitro observations (see Fig. 4*R*,

and Ref. 50a) have shown extensive direct contacts between microvascular pericytes and their coordinated EC (gap junctions characterized by connexin 43 and peg-and-socket contacts), so that directly coupled pericyte and EC(s) very probably constitute a reactive unit.

New Insights into the Cytoarchitecture of Isolated Postcapillary Venules from Human Myocardium

Postcapillary venules, too, were characterized by a continuous endothelial tube and an adventitial pericyte coat, although the latter existed typically as a wide-meshed network (Fig. 6, *A* and *C*). This characteristic morphology of the venular pericyte coat has been described for the first time for postcapillary venules from the frog bladder (82). The net-like arrangement of the venular pericytes in human ventricular myocardium is in accord with the central role of postcapillary venules with regard to their central role in the recruitment of immune defense and inflammation (1, 25, 56). Consistent with their fragile-looking morphology, proteolytic perfusion of the heart ventricles resulted first in the selective disintegration of these vessels. This accidental discovery was subsequently of considerable advantage for harvesting highly enriched fractions of venular segments by continuous through-flow centrifugation during the proteolytic perfusion process.

New Anatomical Model of the Smallest Functional Unit of the Coronary Microcirculation

Figure 10 summarizes in a simplified form our findings on the structure of the smallest functional units of the coronary circulation, comprising the end of a muscular arteriole (red arrow) giving rise to a precapillary arteriole and the latter's capillary system that discharges into a postcapillary venule. The situation is more complex in situ, since one muscular arteriole in the human myocardium normally gives rise to several endarterioles, the capillary systems of which are also interconnected and often drain into different postcapillary venules. Consistent with early findings (82), in the capillary fraction after density gradient centrifugation of isolated coronary microvessels we frequently observed pericytes connected, bridge-like, to distant capillaries, hence, "belonging" to more than one capillary system.

Purification of Constituent Wall Cells of the Smallest Myocardial Arterioles and Venules and Reconstruction of the Microvascular Vessel Walls In Vitro

As far as we are aware, the establishment of extremely pure cultures of EC and pericytes of arteriolar and/or venular origin in the present study is a novelty. While methods for isolating and cultivating venular EC have been reported (49, 59), there is no indication in those studies of the degree of purity, nor is there convincing proof for the venular origin of the resulting cultures, despite the availability of specific markers (19). The same holds for the sole report on the isolation of arteriolar EC (together with cells of venular origin; Ref. 73). Indeed, without the specially developed techniques, we were not able to obtain homogenous cultures of these highly specialized EC. With respect to the pericytes, we were not able to reproduce the results of studies employing selective growth media to obtain pure cultures of these cells (61). Details of the successful isolation and identification of bulk amounts of these cells are described elsewhere (50a).

Employing the Transwell cell culture system, we were able to establish sandwich cultures as described recently (50), with EC on the one side of the filter-like substrate and the appropriate pericytes on the other. Readily realized double staining

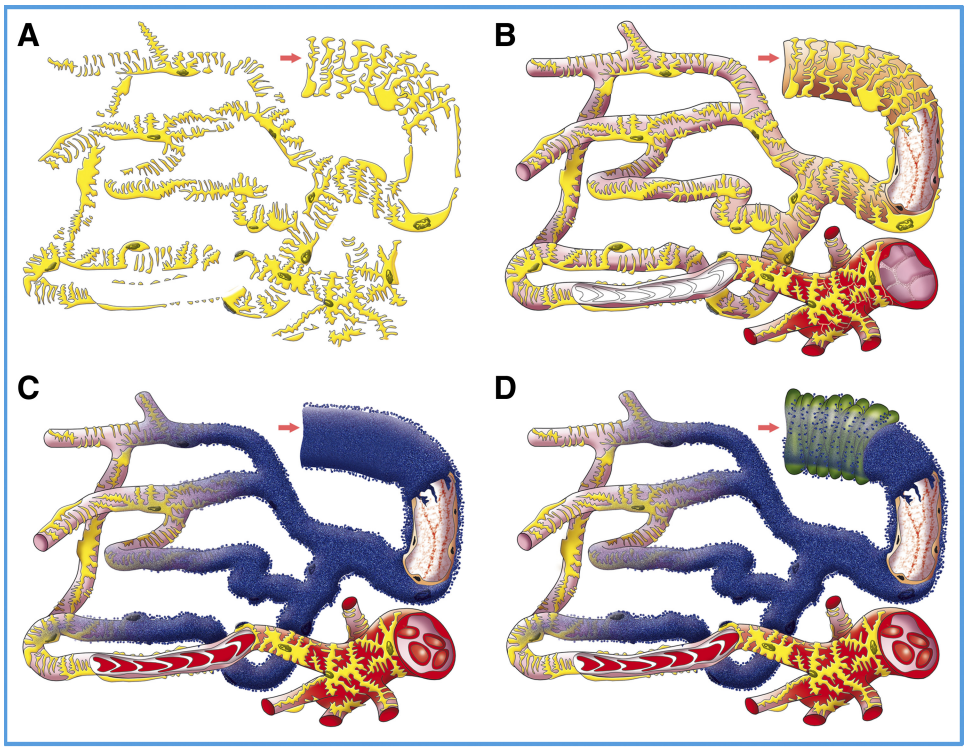

Fig. 10. Schematic stepwise assembly of a smallest functional unit of the coronary microcirculation. *A*: network of interconnected pericytes (yellow). *B*: inclusion of the appropriate endothelial tube segments, which comprise the precapillary arteriolar endothelial tube (cream color, *top right*), the following endothelial tubes of the capillaries (cream to pink) and the endothelial tissue within a postcapillary venule (red, *bottom right*). *C*: extension of the AP-positive, microparticle-containing ECM (blue) in this network. *D*: typically abrupt appearance of SMC (green) at the transition from the precapillary arteriole to muscular arteriole. In principle, the precapillary arteriolar central tube continues upstream into the large coronary arteries.

for the marker enzymes AP and DAP with bright-field or phase-contrast microscopy allowed the state of the cultures to be monitored simply. The apparatus (Fig. 8*B*) developed for the measurement of the hydraulic conductivity and selectivity indices for the transmural movement of various solutes also allowed the cultures to adapt to the plasma-like incubation medium and the routine hydrostatic pressure gradients. The latter are known to influence the initial water transport substantially (3). The gravimetric measurement of filtration rates using a computer-controlled electronic microbalance allowed continuous registration of the filtration rate, and alterations thereof could be detected with an accuracy of <100 μl.

With respect to the comparison between the pericytes of arteriolar and venular origin, we noticed that the latter began to express AP soon after their separation from their EC, although this marker is not normally present in the venular wall. In sandwich cultures with venular EC, however, this enzyme activity rapidly disappeared again. Since direct contact between the EC and pericytes through filter pores during the establishment of the sandwich cultures (during 1 wk) could definitely be excluded (we dealt with unstimulated cells and the ECM of the pericytes prevented apparently the penetration of pericyte processes at least in the routinely prepared sandwich cultures), the mutual influence exerted by these cell types in the sandwich cultures on each other's degree of differentiation is mediated by release products. Indeed, we showed recently that luminal EC and the coordinated subendothelial pericytes in the intima of large human veins exert a strong mutual influence on each other with respect to growth and proliferation (32), if they were cocultured in the sandwich manner.

Basic Filtration Studies and Perspectives

The initial experiments with our in vitro models of terminal arteriolar or postcapillary venular vessel walls showed very clearly that the arteriolar wall is a practically impenetrable barrier with respect to L_P and albumin permeability, irrespective of the presence or absence of inflammatory mediators (as in serum). The venular wall model, on the other hand, behaved very differently. Apart from the generally higher L_P, the degree of tightness decreased rapidly on replacing plasma-like medium by serum-supplemented medium (naturally containing inflammatory mediators). This was consistent with our studies on the influence of platelet- and neutrophil-derived platelet-activating factor and leukotriene LTB_4 on the barrier function of our in vitro models (32a) and the wide, impressively selective opening of the venular endothelial intercellular clefts not only in this model but also in the postcapillary venules in inflamed tissue regions (where serum is always present), thus initiating the development of inflammatory edema (11, 46).

The basal L_P of tissue barriers of precapillary arteriolar origin (SC-PAO; $3.24 \pm 0.52 \cdot 10^{-8} cm \cdot s^{-1} \cdot cmH_2O^{-1}$; $n = 37$) was an order of magnitude lower than that of sandwich cultures of EC and pericytes of postcapillary venular origin (SC-PVO; $2.55 \pm 0.32 \cdot 10^{-7} cm \cdot s^{-1} \cdot cmH_2O^{-1}$; $n = 10$) in plasma-like medium. This was probably due to the higher degree of organization of the intercellular junctions of the arteriolar endothelium and the presence of a thick and continuous ECM organized by the arteriolar pericytes below the endothelial sheet.

Endothelial junctions in venules proved to be generally less organized than those of the arteriolar endothelium (62–64), and permeability studies on isolated venules (54, 77, 79, 80) and arterioles (30, 38) revealed that isolated venules were more leaky than isolated arterioles. We therefore conclude that the observed features of our two in vitro models principally reflect the situation in the respective intact vessels. The higher permeability of venular walls is, in our opinion, less a matter of their physical properties but rather reflects the extraordinary activatability and contractility of their peculiar endothelium. This normally quite tight tissue barrier, specialized for the exchange of cells and macromolecules (1, 25), expresses conspicuously high levels of contractile proteins (7, 17, 18, 41, 70, 71, 81, and this study), the function of which in the cell is enhanced strongly during contact with diverse inflammatory mediators (23, 25–27). In short, venular permeability is more strongly controlled by biochemical mechanisms than many microperfusion studies have suggested. On the other hand, the arteriolar endothelium cannot readily be perturbed and its barrier functions are mainly determined by its physical features. It is thus difficult to compare the L_P and SI values from our studies with values from isolated perfused venules and arterioles and to explain the observed dicrepancies. However, in the course of the vessel wall preparations local release of inflammatory mediators and wall microtraumata cannot be excluded, so that the reported L_P values determined for the respective microvessels should be higher than the measured values in our model, at least for the venules. This is obviously the case. One explanation could be that mechanically induced endothelial or intimal microlesions have substantial effects on wall permeability. In our model, even the smallest scissures in the endothelium or irregularities in the cell architecture (e.g., due to minimal contamination by pericytes or SMC) resulted in a measurable increase in permeability (this study). To avoid these problems, our sandwich cultures were allowed to adapt to physiological pressure conditions in a plasma-like (but serum-free) medium for days, while mechanical damage could be largely excluded by the design of the apparatus. It must, however, be taken into consideration that our in vitro flow and shear force conditions are by far not comparable to those in microperfused vessels, nor do we know whether the cultured endothelium has an intact glycocalyx, the existence of which in traditional *EC* cultures is controversial (52).

As implied above, it was very clear that the pericyte layer in the venular model had practically no influence per se on the L_P, in contrast to the situation in the arteriolar model. The low L_P of the latter presumably reflected the functional impact of the dense, AP-containing ECM. Since the L_P for the SC-PVO in human plasma is similar to the L_P for pericytes with ECM from precapillary arterioles, it can be concluded that confluent pericytes plus ECM impart a similar barrier function as a confluent endothelial venular monolayer. However, it should be noted here that the maintenance of fully differentiated, homogenous pericyte tissue required the presence of species-autologous fetal serum in the growth medium as described elsewhere (50a). It is thus possible that the L_P values for homogenous pericyte layers measured in the present study (culture of human pericytes in media supplemented with heterologous FCS) did not correctly reflect their contribution to the observed tightness of the complete arteriolar barriers in vivo.

Perspectives

In the foregoing, we have reported the successful construction of practical, viable, and histologically well-characterized models of the myocardial precapillary arteriolar and postcapillary venular vessel walls that will allow in vitro experiments under defined and reproducible conditions. It thus now seems possible to obtain more detailed information on the transmural transport, metabolism and pharmacological action of relevant substances in these interesting vascular regions. In addition, our preparatory histological studies have generated new insights into the wall structure of human myocardial arterioles and venules, so providing a new basis for planning and interpreting future experiments on the regulation of microvascular blood flow and barrier functions.

ACKNOWLEDGMENTS

We thank M. Buchner, F. Singer, and H. Sima for constant and very helpful technical support. Furthermore, we thank H. Adelsberger and M. Sumser [Dept. of Cellular Physiology, LMU] for help and advice during confocal microscopic studies, and E. Thielke (Dept. of Anatomy, LMU) and E. Köbele and G. Dachs (Hospital of Dental Medicine, LMU) for assistance during scanning electron microscopy. The excellent photographic and artwork of Barbara Nees is also gratefully acknowledged.

GRANTS

This work was supported by the University of Munich, the German Phlebological Society (//www.phlebology.de) and by a grant of the Friedrich-Baur- Stiftung Munich (info@baur-stiftung.de). The funders had no role in study design, data collection and analysis, decision to publish, or preparation of the manuscript.

DISCLOSURES

No conflicts of interest, financial or otherwise, are declared by the author(s).

REFERENCES

1. **Alcaide P, Auerbach S, Luscinskas FW.** Neutrophil recruitment under shear flow: it's all about endothelial cell rings and gaps. *Microcirculation* 16: 43–57, 2009.
2. **Anderson BG, Anderson WD.** Microvasculature of the canine heart demonstrated by scanning electron microscopy. *Am J Anat* 158: 217–227, 1980.
3. **Baetscher M, Brune K.** An in vitro system for measuring endothelial permeability under hydrostatic pressure. *Exp Cell Res* 148: 541–547, 1983.
4. **Bassingthwaighte JB, Yipintsoi T, Harvey RB.** Microvasculature of the dog left ventricular myocardium. *Microvasc Res* 7: 229–249, 1974.
5. **Bechmann I, Galea I, Perry VH.** What is the blood-brain barrier (not)? *Trends Immunol* 28: 5–11, 2007.
6. **Bian K, Murad F.** Nitric oxide (NO)–biogeneration, regulation, and relevance to human diseases. *Front Biosci* 8: d264–278, 2003.
7. **Bogatcheva NV, Verin AD.** The role of cytoskeleton in the regulation of vascular endothelial barrier function. *Microvasc Res* 76: 202–207, 2008.
8. **Brown RE.** The pattern of the microcirculatory bed in the ventricular myocardium of domestic mammals. *Am J Anat* 116: 355–374, 1965.
9. **Cardoso FL, Brites D, Brito MA.** Looking at the blood-brain barrier: molecular anatomy and possible investigation approaches. *Brain Res Rev* 64: 328–363, 2010.
10. **Cui L, Ju Y, Ding L, Trejo-Morales M, Olfert IM.** Arteriolar and venular capillary distribution in skeletal muscles of old rats. *J Gerontol A Biol Sci Med Sci* 63: 928–935, 2008.
11. **Curry FE, Zeng M, Adamson RH.** Thrombin increases permeability only in venules exposed to inflammatory conditions. *Am J Physiol Heart Circ Physiol* 285: H2446–H2453, 2003.
12. **Dejana E, Corada M, Lampugnani MG.** Endothelial cell-to-cell junctions. *FASEB J* 9: 910–918, 1995.
13. **Diaz-Flores L, Gutierrez R, Madrid JF, Varela H, Valladares F, Acosta E, Martin-Vasallo P, Diaz-Flores L Jr.** Pericytes Morphofunction, interactions and pathology in a quiescent and activated mesenchymal cell niche. *Histol Histopathol* 24: 909–969, 2009.
14. **Dore-Duffy P.** Pericytes: pluripotent cells of the blood brain barrier. *Curr Pharm Des* 14: 1581–1593, 2008.
15. **Fernandez-Klett F, Offenhauser N, Dirnagl U, Priller J, Lindauer U.** Pericytes in capillaries are contractile in vivo, but arterioles mediate functional hyperemia in the mouse brain. *Proc Natl Acad Sci USA* 107: 22290–22295, 2010.
16. **Furchgott RF, Zawadzki JV.** The obligatory role of endothelial cells in the relaxation of arterial smooth muscle by acetylcholine. *Nature* 288: 373–376, 1980.
17. **Garcia JG.** Concepts in microvascular endothelial barrier regulation in health and disease. *Microvasc Res* 77: 1–3, 2009.
18. **Garcia JG, Pavalko FM, Patterson CE.** Vascular endothelial cell activation and permeability responses to thrombin. *Blood Coagul Fibrinolysis* 6: 609–626, 1995.
19. **Garlanda C, Dejana E.** Heterogeneity of endothelial cells. Specific markers. *Arterioscler Thromb Vasc Biol* 17: 1193–1202, 1997.
20. **Giatromanolaki A, Sivridis E, Maltezos E, Koukourakis MI.** Down-regulation of intestinal-type alkaline phosphatase in the tumor vasculature and stroma provides a strong basis for explaining amifostine selectivity. *Semin Oncol* 29: 14–21, 2002.
21. **Granger HJ, Schelling ME, Lewis RE, Zawieja DC, Meininger CJ.** Physiology and pathobiology of the microcirculation. *Am J Otolaryngol* 9: 264–277, 1988.
22. **Green HD.** Circulation; physical principles. In: *Medical Physics*, edited by Glasser O. Chicago, IL: Year Book Publishers, 1944, p. 208–232.
23. **Grega GJ.** Contractile elements in endothelial cells as potential targets for drug action. *Trends Pharmacol Sci* 7: 452–457, 1986.
24. **Grega GJ, Adamski SW.** Patterns of constriction produced by vasoactive agents. *Fed Proc* 46: 270–275, 1987.
25. **Grega GJ, Adamski SW.** The role of venular endothelial cells in the regulation of macromolecular permeability. *Microcirc Endothelium Lymphatics* 4: 143–167, 1988.
26. **Grega GJ, Adamski SW, Dobbins DE.** Physiological and pharmacological evidence for the regulation of permeability. *Fed Proc* 45: 96–100, 1986.
27. **Grega GJ, Adamski SW, Svensjo E.** Is there evidence for venular large junctional gap formation in inflammation? *Microcirc Endothelium Lymphatics* 2: 211–233, 1985.
28. **Hammersen F, Hammersen E.** Some structural aspects of precapillary vessels. *J Cardiovasc Pharmacol* 6, *Suppl* 2: S289–303, 1984.
29. **Henrich HA.** Precapillary control of the splanchnic vascular bed. *J Cardiovasc Pharmacol* 7, *Suppl* 3: S73–79, 1985.
30. **Huxley VH, Williams DA.** Basal and adenosine-mediated protein flux from isolated coronary arterioles. *Am J Physiol Heart Circ Physiol* 271: H1099–H1108, 1996.
31. **Isakson BE, Duling BR.** Heterocellular contact at the myoendothelial junction influences gap junction organization. *Circ Res* 97: 44–51, 2005.
32. **Juchem G, Weiss DR, Gansera B, Kemkes BM, Mueller-Hoecker J, Nees S.** Pericytes in the macrovascular intima: possible physiological and pathogenetic impact. *Am J Physiol Heart Circ Physiol* 298: H754–H770, 2010.

32a. **Juchem G, Weiss DR, Knott M, Senftl A, Förch S, Fischlein T, Kreuzer E, Reichart B, Laufer S, Nees S.** Regulation of coronary venular barrier function by blood borne inflammatory mediators and pharmacological tools: insights from novel microvascular wall models. *Am J Physiol Heart Circ Physiol*. Published online ahead of print November 11, 2011; doi:10.1152/ajpheart.00360.2011.

33. **Kaimovitz B, Lanir Y, Kassab GS.** A full 3-D reconstruction of the entire porcine coronary vasculature. *Am J Physiol Heart Circ Physiol* 299: H1064–H1076, 2010.
34. **Kamouchi M, Ago T, Kitazono T.** Brain Pericytes: Emerging Concepts and Functional Roles in Brain Homeostasis. *Cell Mol Neurobiol* 2010.
35. **Kassab GS, Fung YC.** Topology and dimensions of pig coronary capillary network. *Am J Physiol Heart Circ Physiol* 267: H319–H325, 1994.
36. **Kassab GS, Lin DH, Fung YC.** Morphometry of pig coronary venous system. *Am J Physiol Heart Circ Physiol* 267: H2100–H2113, 1994.
37. **Kassab GS, Rider CA, Tang NJ, Fung YC.** Morphometry of pig coronary arterial trees. *Am J Physiol Heart Circ Physiol* 265: H350–H365, 1993.
38. **Kimura M, Dietrich HH, Huxley VH, Reichner DR, Dacey RG Jr.** Measurement of hydraulic conductivity in isolated arterioles of rat brain cortex. *Am J Physiol Heart Circ Physiol* 264: H1788–H1797, 1993.

39. **Krueger M, Bechmann I.** CNS pericytes: concepts, misconceptions, and a way out. *Glia* 58: 1–10, 2010.
40. **Kutcher ME, Herman IM.** The pericyte: cellular regulator of microvascular blood flow. *Microvasc Res* 77: 235–246, 2009.
41. **Lai CH, Kuo KH, Leo JM.** Critical role of actin in modulating BBB permeability. *Brain Res Brain Res Rev* 50: 7–13, 2005.
42. **Ley K, Laudanna C, Cybulsky MI, Nourshargh S.** Getting to the site of inflammation: the leukocyte adhesion cascade updated. *Nat Rev Immunol* 7: 678–689, 2007.
43. **Lunkenheimer PP, Merker HJ.** Distribution of alkaline phosphatase in the microcirculatory pathways of the coronary system. *Acta Histochem* 57: 14–19, 1976.
44. **Mall F.** Die blut-und lymphwege im dünndarm des hundes. *BerKönigl SächsGes Wiss* 14: 151–189, 1888.
45. **Mayhan WG.** Regulation of blood-brain barrier permeability. *Microcirculation* 8: 89–104, 2001.
46. **McDonald DM.** Endothelial gaps and permeability of venules in rat tracheas exposed to inflammatory stimuli. *Am J Physiol Lung Cell Mol Physiol* 266: L61–L83, 1994.
47. **Michel T, Vanhoutte PM.** Cellular signaling and NO production. *Pflügers Arch* 459: 807–816, 2010.
48. **Moss DW.** Release of membrane-bound enzymes from cells and the generation of isoforms. *Clin Chim Acta* 226: 131–142, 1994.
49. **Moyer CF, Dennis PA, Majno G, Joris I.** Venular endothelium in vitro: isolation and characterization. In Vitro *Cell Dev Biol* 24: 359–368, 1988.
50. **Nakagawa S, Deli MA, Nakao S, Honda M, Hayashi K, Nakaoke R, Kataoka Y, Niwa M.** Pericytes from brain microvessels strengthen the barrier integrity in primary cultures of rat brain endothelial cells. *Cell Mol Neurobiol* 27: 687–694, 2007.

50a. **Nees S, Weiss DR, Senftl A, Knott M, Förch S, Schnurr M, Weyrich P, Juchem G.** Isolation, bulk cultivation, and characterization of coronary microvascular pericytes: the second most frequent myocardial cell type in vitro. *Am J Physiol Heart Circ Physiol*; published ahead of print October 28, 2011, doi:10.1152/ajpheart.00359.2011.

51. **Nourshargh S, Marelli-Berg FM.** Transmigration through venular walls: a key regulator of leukocyte phenotype and function. *Trends Immunol* 26: 157–165, 2005.
52. **Potter DR, Jiang J, Damiano ER.** The recovery time course of the endothelial cell glycocalyx in vivo and its implications in vitro. *Circ Res* 104: 1318–1325, 2009.
53. **Powell T, Twist VW.** A rapid technique for the isolation and purification of adult cardiac muscle cells having respiratory control and a tolerance to calcium. *Biochem Biophys Res Commun* 72: 327–333, 1976.
54. **Qiao RL, Sadurski R, Bhattacharya J.** Hydraulic conductivity of ischemic pulmonary venules. *Am J Physiol Lung Cell Mol Physiol* 264: L382–L386, 1993.
55. **Rao RM, Yang L, Garcia-Cardena G, Luscinskas FW.** Endothelial-dependent mechanisms of leukocyte recruitment to the vascular wall. *Circ Res* 101: 234–247, 2007.
56. **Rodrigues SF, Granger DN.** Role of blood cells in ischaemia-reperfusion induced endothelial barrier failure. *Cardiovasc Res* 87: 291–299, 2010.
57. **Romanul FC, Bannister RG.** Localized areas of high alkaline phosphatase activity in the terminal arterial tree. *J Cell Biol* 15: 73–84, 1962.
58. **Sainte-Marie G.** The lymph node revisited: development, morphology, functioning, and role in triggering primary immune responses. *Anat Rec* 293: 320–337, 2010.
59. **Schelling ME, Meininger CJ, Hawker JR Jr, Granger HJ.** Venular endothelial cells from bovine heart. *Am J Physiol Heart Circ Physiol* 254: H1211–H1217, 1988.
60. **Serban DN, Nilius B, Vanhoutte PM.** The endothelial saga: the past, the present, the future. *Pflügers Arch* 459: 787–792, 2010.
61. **Shepro D, Morel NM.** Pericyte physiology. *FASEB J* 7: 1031–1038, 1993.
62. **Simionescu M, Simionescu N, Palade GE.** Characteristic endothelial junctions in different segments of the vascular system. *Thromb Res* 8: 247–256, 1976.
63. **Simionescu M, Simionescu N, Palade GE.** Segmental differentiations of cell junctions in the vascular endothelium. Arteries and veins. *J Cell Biol* 68: 705–723, 1976.
64. **Simionescu M, simionescu N.** Ultrastructure of the microvascular wall: functional correlations. In: *Handbook of Physiology. The Cardiovscular System.* Bethesda, MD: Am Physiol Soc, 1984, sect 2, vol IV, part 1, p. 41–101.
65. **Sims DE.** Recent advances in pericyte biology–implications for health and disease. *Can J Cardiol* 7: 431–443, 1991.
66. **Suttorp N, Hessz T, Seeger W, Wilke A, Koob R, Lutz F, Drenckhahn D.** Bacterial exotoxins and endothelial permeability for water and albumin in vitro. *Am J Physiol Cell Physiol* 255: C368–C376, 1988.
67. **Suttorp N, Polley M, Seybold J, Schnittler H, Seeger W, Grimminger F, Aktories K.** Adenosine diphosphate-ribosylation of G-actin by botulinum C2 toxin increases endothelial permeability in vitro. *J Clin Invest* 87: 1575–1584, 1991.
68. **Thurston G, Baluk P, McDonald DM.** Determinants of endothelial cell phenotype in venules. *Microcirculation* 7: 67–80, 2000.
69. **Tilton RG.** Capillary pericytes: perspectives and future trends. *J Electron Microsc Tech* 19: 327–344, 1991.
70. **Valeski JE, Baldwin AL.** Role of the actin cytoskeleton in regulating endothelial permeability in venules. *Microcirculation* 10: 411–420, 2003.
71. **Victorino GP, Newton CR, Curran B.** Modulation of microvascular hydraulic permeability by platelet-activating factor. *J Trauma* 56: 379–384, 2004.
72. **Voisin MB, Probstl D, Nourshargh S.** Venular basement membranes ubiquitously express matrix protein low-expression regions: characterization in multiple tissues and remodeling during inflammation. *Am J Pathol* 176: 482–495, 2010.
73. **Wagner L, Hoey JG, Erdely A, Boegehold MA, Baylis C.** The nitric oxide pathway is amplified in venular vs arteriolar cultured rat mesenteric endothelial cells. *Microvasc Res* 62: 401–409, 2001.
74. **Weibel ER.** On pericytes, particularly their existence on lung capillaries. *Microvasc Res* 8: 218–235, 1974.
75. **Wiedeman MP.** Dimensions of blood vessels from distributing artery to collecting vein. *Circ Res* 12: 375–378, 1963.
76. **Wilhelm I, Fazakas C, Krizbai IA.** In vitro models of the blood-brain barrier. *Acta Neurobiol Exp (Warsz)* 71: 113–128, 2011.
77. **Wu HM, Yuan Y, Zawieja DC, Tinsley J, Granger HJ.** Role of phospholipase C, protein kinase C, and calcium in VEGF-induced venular hyperpermeability. *Am J Physiol Heart Circ Physiol* 276: H535–H542, 1999.
78. **Yamagishi S, Imaizumi T.** Pericyte biology and diseases. *Int J Tissue React* 27: 125–135, 2005.
79. **Yuan Y, Chilian WM, Granger HJ, Zawieja DC.** Permeability to albumin in isolated coronary venules. *Am J Physiol Heart Circ Physiol* 265: H543–H552, 1993.
80. **Yuan Y, Granger HJ, Zawieja DC, Chilian WM.** Flow modulates coronary venular permeability by a nitric oxide-related mechanism. *Am J Physiol Heart Circ Physiol* 263: H641–H646, 1992.
81. **Yuan Y, Huang Q, Wu HM.** Myosin light chain phosphorylation: modulation of basal and agonist-stimulated venular permeability. *Am J Physiol Heart Circ Physiol* 272: H1437–H1443, 1997.
82. **Zimmermann KW.** Der feinere Bau der Blutcapillaren. *Zeitschr f d ges Anat* 68: 29–109, 1923.